A case study of performance comparison between vacuum preloading and fill surcharge for soft ground improvement

By

Dao-Yuan TAN (Professor)

School of Earth Sciences and Engineering

Nanjing University, Nanjing, China
Email: rztdy2009@gmail.com

Hong-Tao HE (Senior Engineer)
CCCC-FHDI Engineering Co.,Ltd., Haizhu District, Guangzhou, China
Email: heht@fhdigz.com

Kai LIU (Research Assistant Professor, Corresponding Author)
Department of Civil and Environmental Engineering
The Hong Kong Polytechnic University, Hung Hom, Kowloon, Hong Kong, China
Tel: (852) 5578 3287, Fax: (852) 2334 6389
Email: kevin.kai.liu@hotmail.com; kevin-kai.liu@connect.polyu.hk

Wei-Qiang FENG (Assistant Professor)
Department of Ocean Science and Engineering
The Southern University of Science and Technology, Shenzhen, China
Email: fengwq@sustech.edu.cn

Hong-Hu ZHU (Professor)
School of Earth Sciences and Engineering
Nanjing University, Nanjing, China
Email: zhh@nju.edu.cn

Jian-Hua YIN (Chair Professor)
Department of Civil and Environmental Engineering
The Hong Kong Polytechnic University, Hung Hom, Kowloon, Hong Kong, China
Email: cejhyin@polyu.edu.hk

Manuscript submitted to *International Journal of Geosynthetics and Ground Engineering* for possible publication as a Case Study

Oct 2023

Abstract

Vacuum preloading and fill surcharge are two common ground improvement methods, which have been successfully utilized in many soil improvement and land reclamation projects all over the world. Therefore, continuous study on them is of great necessity for deepening the research for both optimizing the solution of treating soft grounds and predicting the deformation performance. This paper presents a case study of a land reclamation project, in which both vacuum preloading and fill surcharge methods were compared based on the detailed field monitoring data, in-situ and laboratory tests of two selected areas treated with well-controlled construction quality. The results indicate that the vacuum preloading method can accelerate the consolidation progress more effectively and exhibit better performance in reducing the water content of soft soils. In this method, a stable vacuum pressure was kept beneath the air-tight membrane, and the bentonite-slurry cut-off walls were installed surrounding the treated land to prevent the vacuum leakage throughout permeable interlayers. However, the vacuum pressure decreased significantly along the depth, which affected the efficiency of improving the deeper soil layer. On the other hand, the fill surcharge method can accelerate consolidation and improve the strength of soft soils in a relatively slow but predictable way. Furthermore, four different methods are adopted to predict the ultimate settlements of ground in this study, including Asaoka's method, hyperbolic curve method, exponential curve method, and new simplified B method. In general, good performance of the four methods can be observed by comparing measured and predicted settlements.

Keywords: Ground improvement; Vacuum preloading; Fill surcharge; Soft soil; new simplified B method

Introduction

Soft clayey soils with thick layers are widely distributed along the south coast of China. These soft soil layers normally have high water content, high compressibility, low strength, and significant creep behavior, which have led to various problems to the development of underground space [1–8]. To provide a potential solution for the increasing demand or new lands for continuous urbanization, soft soils in those coastal lands were treated to obtain sufficient strength and stiffness for the development of infrastructure [9–11]. Therefore, various ground improvement methods are developed and commonly adopted to achieve this objective. Table 1 classifies the state-of-art techniques for soft soil improvement. Among those techniques, the most direct way to improve saturated soft soils is by reducing the water content through consolidation, which refers to an increase of the effective stress [12]. Based on Terzaghi's effective stress principle, increasing total stress and reducing pore-water pressure can be achieved by applying fill surcharge and vacuum preloading, respectively. Under vacuum pressure, the pore-water pressure in the soil layer decreases from the hydro-static state, which results in an increase of the effective stress by the magnitude of the reduced pore-water pressure [13]. Furthermore, applying a surcharge pressure will significantly increase the pore-water pressure from the hydro-static state at first, and dissipation of excess pore pressure leads to an increase of the effective stress and a reduction of the water content [14, 15].

The vacuum preloading method was first introduced by Kjellman [16] of the Swedish Geotechnical Institute. Since then, this method has been developed into a mature technique for the improvement of soft grounds and successfully utilized quite extensively all over the world [17–23]. Fill surcharge preloading is one of the simplest methods for ground improvement. It has been commonly used for soft soil treatment [24–28]. Prefabricate vertical drains (PVDs)

are usually utilized to accelerate consolidation of soft soils and shorten the dissipation path of the excess pore water for both two methods. These two methods have been developed to provide vacuum load, which are the air-tight sheet method (membrane system) and the direct vacuum-drain method (membraneless system) [12].

In order to evaluate and optimize the different soil improvement techniques, it is necessary to calculate the degree of consolidation, which requires the prediction of ultimate settlements of improved ground. It is challenging to accurately predict the ultimate settlement since the soft soil has high water content and high compressibility. In general, the conventional simplified settlement calculations are based on Terzaghi's 1D consolidation equations, which ignore the creep effect of soil. The time-dependent settlements are normally divided into two parts, including "primary" consolidation due to dissipation of excess pore-water pressure and "secondary" consolidation induced by viscous soil skeleton. Initially, creep was considered as the "secondary" consolidation which occurs after the "primary" consolidation in "Hypothesis A". However, the "Hypothesis A" was questioned since it does not align with the developing theories on the viscous behaviours of clayey soils and often underestimates long-term settlements [29]. "Hypothesis B" suggested that creep can happen even during the "primary" consolidation [30].

The development of Hypothesis B mainly includes two phases, in which predictions of degree of consolidation and creep deformation are involved. In the first phase, degree of consolidation with time was predicted, in which Terzaghi's 1D consolidation equations were developed. However, some problems cannot be directly considered, such as multi-stage and ramp loadings and multi-layered soils. A series of studies have been conducted to consider the multi-layered

soils based on analytical and numerical methods [31, 32]. The second phase of Hypothesis B involved the prediction of creep deformation with time based on elastic visco-plastic constitutive models. Yin and Graham [33, 34] proposed a concept of “equivalent time line” for modelling the time-dependent behaviour of clays. These models were further improved to describe 3D stresses [35, 36]. The traditional methods require complex concepts and may suffer from non-convergence problems; therefore, simplified handy methods were developed to predict settlement of single or multi-layered soft soils [37–39]. However, there is a lack of validations for these simplified handy methods, especially for the case studies in which different types of soil improvement techniques such as vacuum preloading and fill surcharge methods in one construction site.

In engineering practice, the ultimate settlement is usually estimated based on some observational methods, such as Asaoka's method [40], hyperbolic curve method [41–43], and exponential curve method [44, 45]. These methods have been used to predict settlements based on the observational data of settlement. The values of parameters in these methods are subject to influences of factors, including time interval, initial calculation point, etc. Thus, the soil parameters derived from the measured settlements might be variable. The variable parameters might induce a great difference in predicting settlements. Therefore, it is still necessary to evaluate and analyse these observational methods and compare the simplified handy and observational methods based on field data.

In this paper, a case study of comparing the effectiveness of vacuum preloading and fill surcharge methods in improving the properties of soft soils is reported. The background of the studied project and the adopted soil improvement techniques are described in detail. The

vacuum pressures/surcharge fill heights, multi-level settlements, and pore-water pressures were monitored during consolidation of the treated soft grounds. The performances of the used ground improvement methods are evaluated based on the real-time responses of the pore-water pressure and ground settlement to the application of the vacuum pressure/surcharge load. Besides, to estimate the ultimate settlement, four different methods are adopted and compared with the measured settlements in the field, which are more accurate than those simulated settlements in the previous studies.

Background of the Project

The studied project belongs to the construction project of a coastal resort in Zhuhai, China, as shown in Figure 1(a). The area of the treated land is around 54 *ha*. Specifically, 25 *ha* was improved by the fill surcharge method, and the other 29 *ha* was treated by the vacuum preloading method. For the fill surcharge method, the ground is divided into different zones with the area varying from 1.8 to 6.7 *ha*. For the vacuum preloading method, the block area treated each time is smaller to control the quality of the vacuum preloading distribution, which varies from 1.6 to 3.8 *ha*. In addition, in-situ bentonite-slurry cut-off walls were installed surrounding each treated block for sealing the treated soft ground and preventing the effects of permeable interlayers. Prefabricated vertical drains (PVDs) were used in both methods to accelerate consolidation and reduce the drainage pathway.

Instrumentation of the study area for ground improvement is presented in Figure 1(a). Independent monitoring of each district was adopted for individual assessment of soil improvement quality. Figure 1(b) shows a typical example of the arrangement of important instruments in one district. Specifically, a settlement plate was placed on the sand layer for the

monitoring of ground settlement. A magnetic extensometer was installed in a borehole for the monitoring of the multi-level settlement. The distance between neighbouring settlement rings was kept at 4 m. Similarly, a series of pore water pressure transducers, vibrating wire piezometers, were also installed at different depths with a constant interval of 4 m in each district to measure the pore-water pressure variations of improved soil. The major components of the vibrating wire piezometer include pressure sensitive stainless steel diaphragm and vibrating wire element [46]. The negative pore-water pressure can be measured since the negative pressure can change the tension in the wire and then causes a shift of natural vibrating frequency. The high air entry value of ceramic cups used on the vibrating wire piezometer is 300 kPa. The monitoring data of those transducers in the selected districts are plotted and analysed in this study.

According to the geotechnical investigations, the thickness of the revealed soil layers at the site is more than 30m, and these layers include fill, mud, clay-silty clay, mucky soil, residual soil. Figure 2 illustrates a typical soil profile with essential geotechnical engineering properties. The depth of ground water table was around 1.5 m. The natural water content was 40% - 90%, greater than the liquid limit of the corresponding soil layer. The soil weight ranged from 14 to 19 kN/m^3. The void ratio was 1.000 - 2.200. The coefficients of consolidation in the vertical direction ($c_{v,1-2}$) and the horizontal direction ($c_{h,1-2}$) for pressure ranging from 100 kPa to 200 kPa, the coefficients of permeability for pressure ranging from 100 kPa to 200 kPa in the vertical direction ($k_{v,1-2}$) and the horizontal direction ($k_{h,1-2}$) are also plotted in Figure 2 as a valuable reference. The similar values for coefficients of consolidation and permeability under different directions probably showed slight soil anisotropy effect in the deposition. In general, the coefficients of volume compressibility decreased with the increase of depth. The bedrock

level is very fluctuant for the area with granite bedrock; thus, the thickness of soft soil might be different in different locations on the site. This study focuses on the soft ground improvement; thus, the borehole exposed bedrock is not shown in the typical soil profile.

Ground Improvement Procedures

For the ground improvement project, there are several design requirements to be fulfilled. The ground elevation after ground improvement shall be at +3.5 m. The bearing capacity of soil based on static loading test shall not be less than 120 kPa. Before starting the ground improvement work, a layer of geotextile (tensile strength higher than 40 kN/m), a layer of geogrid (tensile strength higher than 175 kN/m), a 0.7-m-thick medium-coarse sand layer, and a 0.7-m-thick fine-medium sand layer were placed on the ground surface. PVDs were then installed on a square grid at a spacing of 1.1 m. The PVDs were designed to penetrate the treated soft soil layers and be inserted into the underlying clay layer for at least 0.3 m. Following this criterion, the embedded depth of the PVDs ranged between 16 to 30 m.

Vacuum preloading method

As mentioned, before the adoption of the vacuum pressure, PVDs were installed for distributing vacuum load and discharging pore-water pressure. The air-tight sheet method was adopted. Because the soil layers are mainly clayey soils with low permeability, a higher effective vacuum pressure can be reached using this method with the help of bentonite-slurry cut-off walls surrounding the ground to be treated [47]. These cut-off walls can be used to avoid the loss of the vacuum pressure due to the inter-bedded permeable layers. A sand layer was placed on the ground surface for linking the PVDs to the main vacuum pressure lines. Three layers of membrane were placed on the ground surface to seal the treated ground and covered by a water

layer. The schematic layout of the vacuum preloading method is presented in Figure 3. The perforated depths of PVD were classified by different zones in Figure 1(a) based on the depths of the clay layers underneath the soft soils, i.e., the PVDs were penetrated through the soft soil layers and driven into the stiffer clay layer underneath for around 30 cm. Thus, the vacuum pressure can be applied in a controlled manner. The vacuum loading under the membrane was kept at least 85 kPa for more than 90 days. For the vacuum preloading technique, the analysis of the in-situ monitoring data is an essential part to assess and maintain the effectiveness of vacuum preloading [12]. Therefore, a real-time field monitoring system was established in the treated grounds, as shown in Figure 1.

Fill surcharge method

The aim of the fill surcharge work is to preload the soft ground soil for achieving an effective stress larger than the designed workloads, which was 40 kPa in this case. Thus, the surcharge pressure was determined as 65 kPa based on the estimated workload on the ground, and the corresponding total thickness of fill material was around 4 m, separated into two stages with 2 m fill in each stage. The schematic layout of the fill surcharge method is presented in Figure 4. After the adoption of the full surcharge load, consolidation was continued for at least another 150 days before removing the surcharge fill.

Measurement and Analysis of Field Data

The instrumentation adopted in this project mainly consists of the monitoring of water level, pore-water pressure, and multi-level settlement. Besides, the water content, undrained shear strength, and in-situ vane shear strengths of soils before and after the ground improvement work were measured by laboratory tests and in-situ vane shear tests.

Settlement

The settlements of the treated ground at different depths were monitored. The monitoring data in two typical zones based on two different methods are plotted in Figure 5. From the settlement data, the average degree of consolidation (DOC), U_{avg}, during the soil treatment is calculated as the ratio of the current settlement to the ultimate settlement [18]. The ultimate settlement here is predicted using the widely accepted Asaoka's method proposed by Asaoka [40]. Figure 5(a) shows the development of the settlements and the degree of consolidation against the fill surcharge load in Zone D1. It can be noted that the full adoption of the surcharge load cost nearly one month. The data of the ground in Zone D8 treated by the vacuum preloading method is plotted in Figure 5(b). It can be observed that the vacuum pressure reached its designed value of 90 kPa in half a month since the vacuum pump started to work. It can be found that the degree of consolidation increased greatly with the adoption of the vacuum pressure in the first 60 days until the DOC reached 72%. The settlement of the ground treated by the fill surcharge method developed more steadily than which treated by the vacuum preloading. As in the fill surcharge method, the vertical total pressure applied by the fill material is uniformly distributed in the soft soils, whereas in the vacuum preloading method, the suction is applied by the vacuum pump, which is highly dependent on the permeability and installation quality of the prefabricated vertical drains (PVDs) for distributing the vacuum load. Before removal of the fill surcharge, the degree of consolidation achieved 78%, and the settlement exceeded 1.5m. Comparing the degrees of consolidation of the two methods, the soil layers treated by the vacuum preloading method reached 70% in more than four months, whereas the fill surcharge method needed nearly 3 months to achieve the same degree of consolidation. However, the DOC in the vacuum preloading treated ground increased much slower than the fill surcharged ground after the first two months due to the unavoidable loss of the vacuum pressure because

of the gradual clogging of the PVDs in field applications and the upper limit of pore-pressure reduction applied by the vacuum preloading technology, which cannot generate a suction higher than 95 kPa in engineering practice [48].

Predictions of ultimate settlement by different methods

(a) Asaoka's method

Mikasa [49] proposed a consolidation equation in terms of strain shown as follows for 1D consolidation problems.

$$\frac{\partial \varepsilon(t,z)}{\partial t} = C_{\mathrm{v}} \frac{\partial^2 \varepsilon(t,z)}{\partial z^2} \tag{1}$$

where $\varepsilon(t,z)$ is the vertical strain, t is the time period, z is the length of drainage path, and C_{v} is the coefficient of consolidation.

Asaoka [40] suggested using a differential equation shown as follows to describe the equation (1):

$$S + a_1 \frac{\mathrm{d}S}{\mathrm{d}t} + a_2 \frac{\mathrm{d}^2 S}{\mathrm{d}t^2} + \cdots + a_n \frac{\mathrm{d}^n S}{\mathrm{d}t^n} = b \tag{2}$$

where S is the total settlement which includes initial compression, primary compression, and secondary compression, a_1, a_2, … a_n, and b are soil constants relate to the coefficient of consolidation and boundary conditions.

The settlement *versus* time curve can be divided into many parts with a same period, Δt. Therefore, equation (2) can be described by the equation as follows:

$$S_j = \beta_0 + \sum_{i=1}^{n} \beta_i S_{j-i} \tag{3}$$

where S_j and S_{j-1} are the settlement at periods of j and j-1, respectively. The coefficients β_0 and β_i are constants.

In general, equations (2) and (3) can be approximately simplified as first-order equations shown as follows in engineering practice:

$$S + a_1 \frac{\mathrm{d}S}{\mathrm{d}t} = b \tag{4}$$

$$S_j = \beta_0 + \beta_1 S_{j-1} \tag{5}$$

Thus, the settlement at period of t, S_t, can be calculated by the equation as follows:

$$S_t = S_\infty - \left(S_\infty - S_0\right) \mathrm{e}^{-\frac{t}{C_1}} \tag{6}$$

$$\ln \beta_1 = -\frac{\Delta t}{C_1} \tag{7}$$

where S_∞ is the ultimate settlement, S_0 is the initial settlement, C_1 is a soil constant, Δt is a constant time interval, and e is the base of natural logarithm. It can be concluded that S_t approaches S_∞ when period, t_j, is infinity. Therefore, the ultimate settlement can be expressed as follows:

$$S_{\infty} = \frac{\beta_0}{1-\beta_1} \quad (8)$$

Based on the procedures introduced by Asaoka [40], a series of points, S_1, S_2, S_3, …., S_n, with the same period, $\Delta t = t_n - t_{n-1}$, on the settlement *versus* time curve can be picked out. Then, these points (S_n, S_{n-1}) and a line of 45° can be plotted in a plane. These points can be assumed on a straight line which gives the intercept, β_0, and slope, β_1. Finally, the intersection of this fitted straight line and the line of 45° defines the ultimate settlement. As shown in the plots of S_j and S_{j-1} in Figures 6, 7, and Table 2, the effect of time interval was investigated by using different time intervals, Δt, including 10, 20, and 30 days. In addition, the measured settlements (S_m) in two typical zones were compared with those of predicted results (S_t) to study the applicability of Asaoka's method in different zones. The measured periods of Zones D1 and D8 are 176 and 115 days, respectively. With the increase of time interval for each zone, the intercept (β_0) increases and slope(β_1) decreases (see Table 2). These trends are consistent with those observed by Zhu et al. [45]. In general, the error (defined as $\frac{|S_t - S_m|}{S_m}$) at a measured period increases with the increasing time interval for two zones. The different trend of error for interval of 30 days in Zone D1 might be due to the adoption of measured period. Overall, to obtain a relatively minor error, the shortest time interval (Δt = 10 days) was adopted in applying Asaoka's method in this study.

As shown in settlement *versus* time curves in Figures 6 and 7, the predicted settlements based on different time intervals generally agree well with the measured settlements in the two zones. The predicted settlements in Zone D1 for different time intervals are slightly overestimated. The predicted settlements in Zone D8 are slightly overestimated for different time intervals if

277 monitoring period is shorter than 70 days. In general, for a monitoring period longer than 70
278 days, the predicted settlements in Zone D8 based on intervals of 10 and 20 days are slightly
279 underestimated, and those on a time interval of 30 days are slightly overpredicted.

280

281 (b) Hyperbolic curve method

282 Tan et al. [41] proposed a hyperbolic curve method to predict the settlement as follows, in
283 which the settlement *versus* time curve was assumed as a hyperbolic curve described as follows.

284 $$S_t = S_0 + \frac{t - t_0}{\alpha + \beta(t - t_0)} \Rightarrow \frac{t - t_0}{S_t - S_0} = \alpha + \beta(t - t_0) \quad (9)$$

285 where S_t is the settlement at the time of t, S_0 is the accumulated settlement at the time period of
286 t_0, and α and β are the intercept and slope of the fitted line in the plot of $(\frac{t - t_0}{S_t - S_0})$ and $(t - t_0)$,
287 respectively (see Figures 8(a) and 8(c)).

288

289 Then, the settlement at the time of t, S_t, can be calculated by the equation as follows:

290 $$S_t = \frac{1}{\beta + \frac{\alpha}{t - t_0}} + S_0 \quad (10)$$

291

292 Based on equation (10), the ultimate settlement, S_∞, can be calculated based on the equation
293 as follows when t approaches infinity:

294 $$S_\infty = \frac{1}{\beta} + S_0 \quad (11)$$

As shown in Figures 8(b) and 8(d), the predicted settlements based on the hyperbolic curve method were compared with those of measured settlements for Zones D1 and D8. In general, predicted settlements agree well with those of measured settlements for Zone D1. For Zone D8, the predicted settlements for periods shorter than 70 days are slightly overestimated, and those for periods longer than 70 days are mainly underestimated. The t_0-values for Zones D1 and D8 were assumed to be 50 and 36 days, respectively. The hyperbolic curve method is normally used for the soil with a degree of saturation greater than 40% [41]. The values of degree of saturation for Zones D1 and D8 were 41.5% and 42.1%, respectively. Table 3 lists the predicted results for the ultimate settlements for Zones D1 and D8 based on the hyperbolic curve method. The measured settlements (S_m) in the two different zones were compared with those of predicted results (S_t) to study the applicability of the hyperbolic curve method. The errors between predicted and measured settlements at periods of 176 and 115 days for Zones D1 and D8 are 1.66% and 3.85%, respectively.

(c) Exponential curve method

Barron et al. [44] developed the consolidation theory for radial consolidation using drain walls. The average degree of consolidation, U_{avg}, can be calculated by the following equation:

$$U_{avg} = 1 - e^{-\beta' t} \tag{12}$$

where e is the base of natural logarithm, t is the time, and β' is a soil parameter which can be determined by the equation as follows:

$$\beta' = \frac{8C_h}{D_e^2 F(n)} \tag{13}$$

where D_e is the equivalent diameter of a unit cell of drain, C_h is the coefficient of consolidation in the horizontal direction, and $F(n)$ is a resistance factor which can be used to consider effects of drainage spacing, smear, and well resistance. The value of $F(n)$ can be obtained based on the equation as follows:

$$F(n) = \frac{n^2}{n^2 - 1} \cdot \ln(n) - \frac{3n^2 - 1}{4n^2} \tag{14}$$

where n is the drain spacing ratio.

Furthermore, U_{avg}, can be calculated by the following equation:

$$U_{\text{avg}} = \frac{S_t - S_{\text{d}}}{S_\infty - S_{\text{d}}} \tag{15}$$

where S_t is the settlement at the time of t, S_∞ is ultimate settlement, and S_{d} is the settlement induced by lateral deformation.

Three groups of values (S_i, t_i) on a settlement *versus* time curve are chosen to calculate the ultimate settlement. The intervals of time, $\Delta t = t_i - t_{i-1}$, are the same for these three groups. The S_∞ and β' can be calculated by the equations as follows:

$$S_\infty = \frac{S_3(S_2 - S_1) - S_2(S_3 - S_2)}{(S_2 - S_1) - (S_3 - S_2)} \tag{16}$$

$$\beta' = \frac{1}{\Delta t} \ln \frac{S_2 - S_1}{S_3 - S_2} \tag{17}$$

335 Thus, the settlement at the time of t, S_t can be calculated based on the equation as follows:

336 $$S_t = (S_\infty - S_\mathrm{d})(1 - e^{-\beta' t}) + S_\mathrm{d} \quad (18)$$

337

338 Table 4 lists the corresponding values of Δt, β', S_∞, S_t, and errors for Zones D1 and D8.
339 Three different time intervals, Δt, were used to predict the ultimate settlements for the two
340 zones. The time points for application of full loading were set as initial time points for the two
341 zones. It shows that the adopted data points have a considerable effect on the predicted results,
342 especially for the results in Zone D8. In general, the error decreases with the increase of time
343 interval. This decreasing trend agrees well with those trends observed by Zhu et al. [45]. The
344 different trend of error for interval of 70 days in Zone D1 might be due to the adoption of
345 measured period. In Zone D1, all the errors are less than 4%. These minor errors indicate the
346 effectiveness of the exponential curve method in predicting the ultimate settlement. In Zone
347 D8, the errors for time intervals of 30 and 40 days are considerable. These greater errors might
348 be induced by the less and unsuitable time interval. Thus, the time interval of 50 days was
349 adopted in the prediction. Figures 9(a) and 9(b) show the comparison of the predicted
350 settlements based on the exponential curve method and those of measured settlements for
351 Zones D1 and D8. It is worth noting that the change of time interval has a greater effect on the
352 predicted settlements in Zone D8. It shows that it is of great importance to try different time
353 intervals in the prediction. It is suggested that the measured period shall be as long as possible
354 for more initial points and time intervals. In addition, different groups of initial points and time
355 intervals might be tried to obtain an accurate ultimate settlement.

356

357 (d) A new simplified B method considering creep limit

As shown in Figure 10, Yin et al. [30] proposed a 1D elastic visco-plastic (EVP) model. The reference time line (λ-line) and instant time line (κ-line) can be determined based on conventional oedometer tests. The visco-plastic strain rate, $\Delta\varepsilon^{vp}$, uniquely corresponds to the current stress-strain state, and can be expressed as follows:

$$\Delta\varepsilon^{vp} = \frac{\frac{\psi_0}{V}\ln\left(\frac{t_0+t_e}{t_0}\right)}{1+\frac{\psi_0}{V\Delta\varepsilon_L}\ln\left(\frac{t_0+t_e}{t_0}\right)} \tag{19}$$

where t_e is equivalent time, $\frac{\psi_0}{V}$ denotes creep coefficient, t_0 denotes reference time which is usually taken as 24 hours or the time at the end of "primary" consolidation; and $\Delta\varepsilon_L$ is creep strain limit.

Figs. 11(a) and (b) show the schematic diagram of the 1D EVP model for calculating creep settlements of normally consolidated and over-consolidated soils, respectively. Dashed curves represent the actual stress-strain paths. Preconsolidation pressure point ($\sigma_p^{'}$, ε_p) is on the reference time line, and can be determined by initial OCR if there is one single loading step. ($\sigma_f^{'}$, ε_f) is the final stress-strain state under stress level of $\sigma_f^{'}$ without considering creep. t_e can be calculated by the equation as follows:

$$t_e = t_{e0} + t = \exp\left[\frac{\Delta\varepsilon_f^{vp}}{\frac{\psi_0}{V}\left(1-\frac{\Delta\varepsilon_f^{vp}}{\Delta\varepsilon_L}\right)}\right] t_0 - t_0 + t$$

$$= \exp\left\{\frac{\left[\left(\varepsilon_f - \varepsilon_p\right) - \frac{\lambda}{V}\log\left(\frac{\sigma_f'}{\sigma_p'}\right)\right]}{\frac{\psi_0}{V}\left(1-\frac{\left(\varepsilon_f - \varepsilon_p\right) - \frac{\kappa}{V}\log\left(\frac{\sigma_f'}{\sigma_p'}\right)}{\Delta\varepsilon_L}\right)}\right\} t_0 - t_0 + t \quad \Delta\varepsilon_f^{vp} < \Delta\varepsilon_L \tag{20}$$

where $\Delta\varepsilon_f^{vp}$ denotes difference between the reference strain, ε_f^r, on the reference time line and the targeted strain, ε_f.

The governing equation for consolidation in Walker's solution [50] is shown as follows:

$$\frac{m_v}{\bar{m}_v}\frac{\partial\bar{u}}{\partial t} = -\left[dT_h\frac{\eta}{\bar{\eta}}\bar{u} - dT_v\left(\frac{\partial}{\partial Z}\left(\frac{k_v}{\bar{k}_v}\right)\frac{\partial\bar{u}}{\partial Z} + \frac{k_v}{\bar{k}_v}\frac{\partial^2\bar{u}}{\partial Z^2}\right)\right] + \frac{m_v}{\bar{m}_v}\frac{\partial\bar{\sigma}}{\partial t} + dT_h\frac{\eta}{\bar{\eta}}w \tag{21}$$

where $\bar{u}$ denotes average pore-water pressure at depth of z, $\bar{\sigma}$ denotes average total stress, η denotes a lumped parameter for consideration of horizontal consolidation, w is water pressure applied on the vertical drains. k_v, m_v, and η are considered as depth-dependent in a piecewise linear way, which are normalized by a reference layer chosen from all layers. The normalized depth parameter Z is calculated by $\frac{z}{H}$, and H is the total thickness of soil. In the spectral method, $\bar{u}(Z,t)$ can be determined by integrating over the whole soil depth with a uniform solution expression and shown as follows:

386 $$\bar{u}(Z,t) \approx u_0 \mathbf{\Phi v E} (\Gamma \mathbf{v})^{-1} \theta \quad (22)$$

387 where u_0 denotes initial reference excess pore pressure, $\mathbf{\Phi} = \left[\phi_1(Z) \quad \phi_2(Z) \quad \cdots \quad \phi_N(Z)\right]$ is
388 formed by a series of linearly independent sinusoidal basis functions $\phi_j(Z)$, $\mathbf{E}$ denotes a
389 diagonal matrix relates to the eigenvalues of $\mathbf{\Gamma^{-1}\Psi}$. $\mathbf{\Gamma}$, $\mathbf{\Psi}$, and $\boldsymbol{\theta}$ are matrices associated with
390 soil parameters at any depth. The eigenvectors associated with each eigenvalue of $\mathbf{\Gamma^{-1}\Psi}$ are
391 used to form the columns of matrix $\mathbf{V}$. *N* denotes the number of terms in $\mathbf{\Phi}$, which is usually
392 set to 30. Additional information on the derivation can be referred to [50, 51].
393
394 To determine the degree of consolidation and the primary consolidation settlements for each
395 layer, various input parameters shall be specified, including geometry parameters of drains,
396 soil layers, vertical and horizontal drainage conditions, permeability, volume compressibility,
397 and vertical ramp loading. The primary consolidation settlements can be calculated as follows:
398 $$S_{primary,i}(t) = U_i(t) S_{f,i} \quad (23)$$

399 where $S_{f,i}$ denotes the final deformation of layer-*i* under incremental stress without coupling
400 of excess pore pressure. Then, S_f of a soil element can be determined as follows:

401 $$S_f = \begin{cases} H \dfrac{\kappa}{V} \ln \dfrac{\sigma_f^{'}}{\sigma_0^{'}} & \text{(for over-consolidation state)} \\ H \dfrac{\kappa}{V} \ln \dfrac{\sigma_p^{'}}{\sigma_0^{'}} + H \dfrac{\lambda}{V} \ln \dfrac{\sigma_f^{'}}{\sigma_p^{'}} & \text{(for normal-consolidation state)} \end{cases} \quad (24)$$

402 where *H* is the layer thickness.
403
404 Each layer of soil is divided into sub-layers with a maximum thickness of 0.5m. $S_{f,i}$ is
405 calculated as follows:

406 $$S_{f,i} = \sum_{k=1}^{\Pi\left(\frac{H_i}{0.5\text{m}}\right)} S_{fi,k} \quad (25)$$

407 where *k* represents the number of sub-layers.

408

409 Based on hypothesis B, creep begins before the end of the "primary" consolidation. The total
410 settlements for each layer consist of two parts as follows, including settlements due to
411 dissipation of excess pore pressure, $S_{primary}(t)$, and those due to creep deformation, $S_{creep}(t)$.

412 $$S(t) = S_{primary}(t) + S_{creep}(t) \quad (26)$$

413 $$S_{creep}(t) = \begin{cases} \alpha U S_{creepf}(t) & t \le t_{EOP} \\ \alpha U S_{creepf}(t) + (1-\alpha U) S_{creepd}(t) & t > t_{EOP} \end{cases} \quad (27)$$

414 where S_{creep} after end of "primary" consolidation (EOP) includes two terms, S_{creepf} and S_{creepd}
415 . S_{creepf} is related to the assumption that creep occurs immediately after the load application
416 within the reference time, without considering dissipation of excess pore pressure, while S_{creepd}
417 corresponds to Hypothesis A, which assumes that creep only occurs after EOP. S_{creepf} and
418 S_{creepd} can be determined by equations as follows:

$$S_{creepf}(t) = H\left[\frac{\frac{\psi_0}{V}\ln\left(\frac{t_0+t_e}{t_0}\right)}{1+\frac{\psi_0}{V\Delta\varepsilon_L}\ln\left(\frac{t_0+t_e}{t_0}\right)} - \Delta\varepsilon_f^{vp}\right] \quad (\text{for } t \ge t_0) \quad (28)$$

$$S_{creepd}(t) = H\left[\frac{\frac{\psi_0}{V}\ln\left(\frac{t_0+t_e}{t_{EOP}}\right)}{1+\frac{\psi_0}{V\Delta\varepsilon_L}\ln\left(\frac{t_0+t_e}{t_{EOP}}\right)} - \Delta\varepsilon_f^{vp}\right] \quad (\text{for } t \ge t_{EOP}) \quad (29)$$

where t_{EOP} denotes the elapsed time at end of "primary" consolidation. It should be noted that for soils under ramp loading $\Delta\sigma'(t)$, $\Delta\varepsilon_f^{vp}(t)$ could be time-dependent during the construction time.

The average consolidation degree for each layer can be calculated by $U_i(t)=1-\frac{\bar{u}_i(t)}{\Delta\sigma_i'(t)}$. If there are more than one loading stages, αU_i in Eq. (27) should be replaced by $\alpha U_{multi,i,j}$ in for layer-*i* at stage-*j* with the following equation:

$$U_{multi,i,j}(t)=1-\frac{\sum_{k=1}^{j}\bar{u}_{i,k}(t)}{\sigma_{i,j}(t)-\sigma_{i0}} \tag{30}$$

where $\bar{u}_{i,k}(t)$ is the average excess pore water pressure of layer-*i* at stage-*j*, $\sigma_{i,j}(t)$ is the loading stage after the *j*-th loading and σ_{i0} is the initial value of *j*-th loading.

As shown in Table 5, soil parameters of new simplified B method were obtained by a series of laboratory tests on samples taken from the construction site, including density tests, permeability tests, oedometer tests, etc. Some soil layers were divided into several sub-layers. Parameters of κ and λ were obtained using the data at the time of end of "primary" consolidation. The three major creep parameters of creep coefficient ψ_0, creep strain limit $\Delta\varepsilon_L$ and reference time t_0 were fitted using method proposed by Chen et al. [38]. Detailed calibration procedures can be referred to Chen et al. [38].

In this study, α-value of 0.8 was adopted since it would be meaningful to use the same α-value in the different cases, and this value was widely used in the previous studies. Figures 12(a) and 12(b) show the settlement curves for Zones D1 and D8 based on the new simplified B method,

respectively. In general, the predicted settlements in different zones are consistent with those of measured settlements. The results show the effectiveness of the new simplified B method in predicting the settlements of soft soil layers under different improvement techniques, such as vacuum preloading and fill surcharge. For Zone D8, the predicted settlement based on the new simplified B method is slightly overestimated. This might be induced by the variability of soil properties and possible disturbance of samples taken from the site. Meanwhile, it is still necessary to refine the adopted soil parameters and extend the monitoring period in the future.

Comparison of predicted settlement results based on different methods

Results of estimated ultimate settlements by different methods are listed in Table 6. The predicted ultimate settlements by the new simplified B method in two different zones are the greatest, whilst those by Asaoka's method are the smallest. The trends of Asaoka's method and hyperbolic curve method are consistent with those observed by Chung et al. [52] and Zhu et al. [45]. Figure 13 shows the comparisons of measured and predicted settlements based on different methods in two different zones. For the two different zones, the predicted settlement results by different methods generally agree well with the measured settlement results. It shows the practicability of these methods in predicting settlements in the ground improvement projects. In Zone D1, the predicted settlements by Asaoka's method are slightly overestimated when the monitoring period is shorter than 150 days. The predicted settlements by hyperbolic and exponential curve methods are generally consistent with each other except for the monitoring period longer than about 170 days. The settlement estimated by the new simplified B method matches well with the measured settlement when it is shorter than 130 days. For the period longer than 130 days, the new simplified B method slightly overpredicts the settlement. In Zone D8, the settlements based on Asaoka's method are slightly overpredicted when the monitoring period is less than about 70 days, and the settlements for monitoring period longer

than 70 days are underestimated a little. For the hyperbolic curve method, the settlements in Zone D8 are generally overpredicted when monitoring periods are shorter than 70 days, and those settlements for monitoring periods longer than 70 days are slightly underestimated. For the exponential curve method, the settlements in Zone D8 are slightly underestimated. The settlement estimated by the new simplified B method is slightly overpredicted. Based on the analysis, longer monitoring periods might be helpful to determine more accurate parameters for these different methods. If a longer monitoring period is available, different initial time points or time intervals might be tried to calculate a more accurate and reliable ultimate settlement.

The observational methods require a certain period of time to obtain necessary parameters for estimating the settlement, however, the new simplified B method can be used to estimate the settlement even when there is no monitored data. The new simplified B method can be widely used to estimate the settlement before the construction, and the estimated results are accurate if the soil parameters obtained from laboratory tests are reliable. In addition, the parameters in observational methods are affected by a series of factors, including time interval, initial calculation point, etc. Thus, the variable soil parameters might induce a great difference in predicting settlements.

The similarities and differences among the different methods for predicting the ultimate settlement are further discussed for engineering practice. For similarities, all of the four methods can be used to estimate ultimate settlements of improved soils. Meanwhile, the Asaoka's method, hyperbolic curve method, and exponential curve method are classified as observational methods. For differences, different methods involve different governing equations and derivation and calculation processes. Besides, the requirements of these methods are different, i.e., three observational methods require monitoring data in the field and the new

simplified B method requires laboratory tests in advance. Beside the above mentioned methods, deep learning algorithms can be developed as a potential alternative for ultimate settlement prediction [53, 54].

Variation of excess pore-water pressure

A major difference between fill surcharge and vacuum preloading is the excess pore-water pressure change. Under fill surcharge, the excess pore-water pressure will immediately rise up by the surcharge pressure from the adoption of fill material, and then gradually dissipate with consolidation. When the vacuum pressure is applied, on the other hand, the excess pore-water pressure will reduce from its initial state by the applied vacuum pressure. To further compare the two applied ground improvement methods in this study, the monitored excess pore-water pressure variations of the ground treated by fill surcharge and vacuum preloading are presented in Figures 14(a) and 14(b), respectively. The excess pore-water pressure variations at different depths in the ground treated by the fill surcharge method are presented in Figure 14(a). From the construction sequence of the fill surcharge work shown in Figure 4, the fill material was applied in two stages. In general, it can be observed that the excess pore-water pressure increased with the adoption of the surcharge load. After the full application of the surcharge loading, the excess pore-water pressure dissipated gradually with time. The decrease of excess pore-water pressure might be induced by the complex construction process. When the preloading was applied, the fill materials were over filled, and then shortly adjusted to the targeted elevation. The total stress was drawn linearly for simplification. From Figure 14(b), the excess pore-water pressures at different depths decreased due to the application of vacuum pressure, which therefore accelerated the consolidation of the soft soils. It can be observed that the vacuum pressure underneath the membrane was maintained at 80 kPa, which has only nearly 10% loss compared with the applied pressure of 90 kPa by the vacuum pump. However,

515 the vacuum pressure sharply decayed to less than 20 kPa at the depth of -8.25 m and -20.25 m,
516 even the bentonite-slurry cut-off walls were installed to seal the boundaries of the treated block.
517 For the data abnormality at -8.52 m, it is probably attributed to the clogging and
518 dysfunctionality of the pore-pressure transducer since the pore pressures at the deeper locations
519 at elevations of -12.25 m and -16.25 m were kept below -40 kPa. On the other hand, the reason
520 of the vacuum loss at the depth of -20.25 m could be the permeable residual soil beneath the
521 treated soft ground and the reduction of the discharge capacity of PVD along its length due to
522 clogging. From the direct comparison of the performance of both methods based on the
523 monitored pore pressure variation after full application of the pre-loads (blue zone), it is found
524 that the surcharge method can provide a constant and stable increase of total vertical stress (43
525 kPa as an example for 77.6 kPa total stress applied by 4.6 m fill) to the soft soil layers in the
526 treated area, but the vacuum method can apply a higher effective stress (decreasing from 80
527 kPa to 40 kPa gradually with the depth) to the depth at -16 m. The comparison results could
528 guide the selection of a suitable soil improvement method based on the depth of soft soils to be
529 treated and the accessibility of fill materials.

530

531 ***Development of soil strength***

532 To assess the effectiveness of the ground improvement methods, in situ vane shear tests were
533 conducted before and after the improvement works. Soil samples were also taken from different
534 depths for conducting unconsolidated-undrained triaxial tests (UU tests). Development of the
535 soil properties and shear strengths by the vacuum preloading method and the fill surcharge
536 method are plotted in Figures 15(a) and 15(b), respectively. It can be found that the vacuum
537 preloading method has a more uniform performance in reducing water content along the depth.
538 In general, the c_{uu}-values for two methods have been enhanced along the depth. The decrease

539 in c_{uu} for soils ranging from 20 to 25 m is consistent with the increase in w-values at the same
540 depths. The results generally agree well with the soil profile showing relatively stiffer clay
541 layers ranging from 20 to 25 m (see Fig. 2). Similarly, c_{uv}-values have been strengthened along
542 the depth. The spikes between 5 and 10 m might be induced by nonuniform and thin sandy
543 layers in the mud layer. Moreover, the intersections for water content, cohesion, and shear
544 strength before and after improvement might be due to the slightly different sampling locations
545 and nonuniform soil layers in the field. This is mainly because that the PVDs can help distribute
546 vacuum pressure and discharge pore water to a deeper zone (-40 kPa at 16 m depth as shown
547 in Figure 14(b)), which can thus accelerate the water drain-out process of the treated soft soil
548 uniformly along the depth. To quantify the performance of the ground improvement work, a
549 simple method is proposed as:

550
$$\mathrm{DOI} = \left| \frac{\int \left[p_a(z) - p_b(z) \right] dz}{\int p_b(z)\, dz} \right| \times 100\% \tag{31}$$

551 where DOI indicates the degree of improvement, p_b and p_a are the compared indicators before
552 and after the ground improvement work, respectively. The integral in the numerator is the
553 difference between the curve of p_b and p_a distributed along the depth, and the integral in the
554 denominator denotes the area between the curve of p_b and the vertical axis representing the
555 depth.

556

557 Using equation (31), the DOIs of the soil properties are calculated and listed in Figure 15. Refer
558 to the data availability and data reliability at different depths, the data within the depth ranging
559 between 5 m and 15 m are used for the DOI assessment of w and c_{uu} by UU tests, and the data
560 within the depth ranging between 0 m to 15 m are adopted for the DOI assessment of c_{uv} by
561 vane shear tests, which are marked as blue zone. By innovatively implementing the DOI value,

562 the efficiency of the vacuum preloading method and fill surcharge method in improving
563 different parameters can be standardized for quantified assessment. Both methods can
564 significantly improve the shear strength of soft clay with the water content between 50% to
565 75%, and the vacuum preloading method with slightly greater DOI-value has a better
566 performance in reducing the water content since it can directly apply suction pressure through
567 the PVD to accelerate the drainage of pore water in the soft soils.

568

569 **Conclusions**

570 A case study of comprehensively assessing the treatment effects of the vacuum preloading
571 method and fill surcharge method on improving soft soils for a land reclamation project was
572 reported, and the treatment effects were comparatively analysed. Based on the data from real-
573 time monitoring, field measurement, and laboratory tests, the following conclusions can be
574 drawn:

575 1) Vacuum loading method can reach its designed load much faster than the surcharge fill
576 method. The pore-pressure reduction in the soil layers beneath the membrane was around
577 90% of the applied vacuum pressure and kept stable during the consolidation process.
578 Suction was generated in the soil layers with the help of the PVDs, which thus effectively
579 increased the degree of consolidation.
580 2) Regarding the growth of the DOC, the soft soils treated by the vacuum preloading method
581 consolidated much faster in the first two months. On the other hand, the fill surcharge
582 method accelerated the consolidation process during the whole treating period (nearly half
583 a year). Therefore, a combination of these two methods in one soft soil treatment project is
584 suggested by applying the vacuum pressure in the first two months and constructing the

surcharge fill afterwards for a faster consolidation and higher DOC, which has already been tried in different projects [25, 28].

3) Overall, the predicted settlements by different methods are consistent with the measured settlements. It can be concluded that these methods are of great practicability in predicting settlements in soil improvement projects. The new simplified B method has been further validated by the monitoring data in a real project based on different soil improvement techniques such as vacuum preloading method and fill surcharge.

4) Based on the field vane shear and laboratory tests, the vacuum preloading method can reduce the water content of the soft soils more uniformly along the depth due to the vacuum suction distributed *via* the PVDs, and the fill surcharge method has a better performance in increasing the shear strength of treated soils.

From this case study, detailed field and laboratory data based on the vacuum preloading and the fill surcharge methods were compared and analysed, which can provide a valuable reference for future study on ground improvement. Based on the comparisons, an appropriate ground improvement method should refer to the major objectives of improving the soft soil layers, and the combination of fill surcharge and vacuum preloading methods can be a better solution by avoiding their drawbacks being utilized individually. Besides, a new simplified B method is firstly validated based on the systematic field and laboratory data of a land reclamation project using the vacuum preloading and fill surcharge methods. Moreover, a series of factors on settlement predictions of observational methods are investigated, including time interval, initial calculation point, etc.

Acknowledgement

The work in this paper is supported by a grant (ZDBS) from The Hong Kong Polytechnic University, China. The Start-up Fund for RAPs under the Strategic Hiring Scheme from PolyU (UGC) (Project ID: P0045938) is also acknowledged. We also acknowledge the supports by a RIF project (Grant No.: R5037-18) and GRF projects (PolyU 152100/20E; PolyU 152130/19E; PolyU 152179/18E； PolyU 152209/17E) from Research Grants Council (RGC) of Hong Kong Special Administrative Region Government of China, the Open Research Project Programme of the State Key Laboratory of Internet of Things for Smart City (University of Macau) (No.: SKL-IoTSC(UM)-2021-2023/ORPF/A19/2022), Research Institute for Sustainable Urban Development of The Hong Kong Polytechnic University (PolyU), and Center for Urban Geohazard and Mitigation of Faculty of Construction and Environment of PolyU. Authors would like to acknowledge the helpful discussions with Dr. Ze-Jian CHEN in The Hong Kong Polytechnic University, China. Authors are also grateful to Mr. Xiong HUANG in the CCCC-FHDI Engineering Co., Ltd. in Guangzhou for his kind help in collecting relevant laboratory test results in this study.

Data Availability Statement

The datasets generated during and/or analysed during the current study are available from the corresponding author on reasonable request.

Declarations

Competing interests: The authors declare no competing interests.

Author contributions

Conceptualization: DYT, KL, WQF, HHZ, JHY; Methodology: DYT, KL, WQF; Formal analysis and investigation: DYT, KL, WQF, HTH; Writing - original draft preparation: DYT, KL; Writing - review and editing: DYT, KL, HTH, WQF, HHZ, JHY; Funding acquisition: DYT, KL, JHY; Resources: HTH, WQF, HHZ, JHY; Supervision: HHZ, JHY.

References

1. Jiang X, Zhu H, Yan Z, et al (2023) A state-of-art review on development and progress of backfill grouting materials for shield tunneling. Dev Built Environ 16(October):100250. https://doi.org/10.1016/j.dibe.2023.100250
2. Li KQ, Yin ZY, Liu Y (2023) Influences of spatial variability of hydrothermal properties on the freezing process in artificial ground freezing technique. Comput Geotech 159(March):105448. https://doi.org/10.1016/j.compgeo.2023.105448
3. Wang P, Yin ZY, Hicher PY, Cui YJ (2023) Micro-mechanical analysis of one-dimensional compression of clay with DEM. Int J Numer Anal Methods Geomech 47(15):2706–2724. https://doi.org/10.1002/nag.3597
4. Liang W, Wu H, Zhao S, et al (2022) Scalable three-dimensional hybrid continuum-discrete multiscale modeling of granular media. Int J Numer Methods Eng 123(12):2872–2893. https://doi.org/10.1002/nme.6963
5. Cheng W, Chen RP, Yin ZY, et al (2023) A fractional-order two-surface plasticity model for over-consolidated clays and its application to deep gallery excavation. Comput Geotech 159(May):105494. https://doi.org/10.1016/j.compgeo.2023.105494
6. Liu K, Yin ZY, Chen WB, et al (2021) Nonlinear model for the stress–strain–strength behavior of unsaturated granular materials. Int J Geomech 21(7):04021103. https://doi.org/10.1061/(asce)gm.1943-5622.0002042
7. Shi XS, Liu K, Yin JH (2021) Analysis of mobilized stress ratio of gap-graded

granular materials in direct shear state considering coarse fraction effect. Acta Geotech 16(6):1801–1814. https://doi.org/10.1007/s11440-020-01107-3

8. Soomro MA, Liu K, Mangnejo DA, Mangi N (2022) Effects of twin excavations with different construction sequence on a brick masonry wall: 3D finite element approach. Structures 41866–886. https://doi.org/10.1016/j.istruc.2022.05.060

9. Xu D, Huang M, Zhou Y (2020) One-dimensional compression behavior of calcareous sand and marine clay mixtures. Int J Geomech 20(9):04020137. https://doi.org/10.1061/(asce)gm.1943-5622.0001763

10. Zhu HH, Liu LC, Pei HF, Shi B (2012) Settlement analysis of viscoelastic foundation under vertical line load using a fractional Kelvin-Voigt model. Geomech Eng 4(1):67–78. https://doi.org/10.12989/gae.2012.4.1.067

11. Zhu HH, Zhang CC, Mei GX, et al (2017) Prediction of one-dimensional compression behavior of Nansha clay using fractional derivatives. Mar Georesources Geotechnol 35(5):688–697. https://doi.org/10.1080/1064119X.2016.1217958

12. Chu J, Indraratna B, Yan S, Rujikiatkamjorn C (2014) Overview of preloading methods for soil improvement. Proc Inst Civ Eng - Gr Improv 167(3):173–185. https://doi.org/10.1680/grim.13.00022

13. Leong EC, Soemitro RAA, Rahardjo H (2000) Soil improvement by surcharge and vacuum preloadings. Géotechnique 50(5):601–605. https://doi.org/10.1680/geot.2000.50.5.601

14. Shi XS, Nie J, Zhao J, Gao Y (2020) A homogenization equation for the small strain stiffness of gap-graded granular materials. Comput Geotech 121103440. https://doi.org/10.1016/j.compgeo.2020.103440

15. Shi XS, Zhao J, Gao Y (2021) A homogenization-based state-dependent model for gap-graded granular materials with fine-dominated structure. Int J Numer Anal

Methods Geomech 45(8):1007–1028. https://doi.org/10.1002/nag.3189

16. Kjellman W (1952) Consolidation of clayey soils by atmospheric pressure. Proceedings of a Conference on Soil Stabilization,. In: Proceedings of a Conference on Soil Stabilization, MIT, Boston, USA. pp 258–263

17. Bergado DT, Jamsawang P, Kovittayanon N, et al (2021) Vacuum-PVD improvement: a case study of the second improvement of soft bangkok clay on the subsiding ground. Int J Geosynth Gr Eng 7(4):1–20. https://doi.org/10.1007/s40891-021-00339-x

18. Chu J, Yan SW (2005) Estimation of degree of consolidation for vacuum preloading projects. Int J Geomech 5(2):158–165. https://doi.org/10.1061/(asce)1532-3641(2005)5:2(158)

19. Feng S, Lei H, Lin C (2022) Analysis of ground deformation development and settlement prediction by air-boosted vacuum preloading. J Rock Mech Geotech Eng 14(1):272–288. https://doi.org/10.1016/j.jrmge.2021.05.006

20. Lei H, Fang Q, Liu J, et al (2021) Ultra-soft ground improvement using air-booster vacuum preloading method: laboratory model test study. Int J Geosynth Gr Eng 7(4):1–12. https://doi.org/10.1007/s40891-021-00332-4

21. Shang JQ, Tang M, Miao Z (1998) Vacuum preloading consolidation of reclaimed land: a case study. Can Geotech J 35(5):740–749. https://doi.org/10.1139/cgj-35-5-740

22. Tang M, Shang JQ (2000) Vacuum preloading consolidation of Yaoqiang Airport runway. Géotechnique 50(6):613–623. https://doi.org/10.1680/geot.2000.50.6.613

23. Wang J, Cai Y, Ma J, et al (2016) Improved vacuum preloading method for consolidation of dredged clay-slurry fill. J Geotech Geoenvironmental Eng 142(11):2–6. https://doi.org/10.1061/(asce)gt.1943-5606.0001516

24. Bo MW, Arulrajah A, Nikraz H (2007) Preloading and prefabricated vertical drains design for foreshore land reclamation projects: A case study. Gr Improv 11(2):67–76.

https://doi.org/10.1680/grim.2007.11.2.67

25. Indraratna B, Rujikiatkamjorn C, Ameratunga J, Boyle P (2011) Performance and prediction of vacuum combined surcharge consolidation at port of brisbane. J Geotech Geoenvironmental Eng 137(11):1009–1018. https://doi.org/10.1061/(asce)gt.1943-5606.0000519

26. Indraratna B, Rujikiatkamjorn C, Balasubramaniam AS, McIntosh G (2012) Soft ground improvement via vertical drains and vacuum assisted preloading. Geotext Geomembranes 3016–23. https://doi.org/10.1016/j.geotexmem.2011.01.004

27. Wang J, Fang Z, Cai Y, et al (2018) Preloading using fill surcharge and prefabricated vertical drains for an airport. Geotext Geomembranes 46(5):575–585. https://doi.org/10.1016/j.geotexmem.2018.04.013

28. Yan SW, Chu J (2005) Soil improvement for a storage yard using the combined vaccum and fill preloading method. Can Geotech J 42(4):1094–1104. https://doi.org/10.1139/t05-042

29. Feng WQ, Yin JH (2017) A new simplified Hypothesis B method for calculating consolidation settlements of double soil layers exhibiting creep. Int J Numer Anal Methods Geomech 41(6):899–917. https://doi.org/10.1002/nag.2635

30. Yin JH, Chen ZJ, Feng WQ (2022) A general simple method for calculating consolidation settlements of layered clayey soils with vertical drains under staged loadings. Acta Geotech 17(8):3647–3674. https://doi.org/10.1007/s11440-021-01318-2

31. Zhu G, Yin JH (2005) Solution charts for the consolidation of double soil layers. Can Geotech J 42(3):949–956. https://doi.org/10.1139/t05-001

32. Xie KH, Xie XY, Jiang W (2002) A study on one-dimensional nonlinear consolidation of double-layered soil. Comput Geotech 29(2):151–168. https://doi.org/10.1016/S0266-352X(01)00017-9

732 33. Yin JH, Graham J (1989) Viscous-elastic-plastic modelling of one-dimensional time-
733 dependent behaviour of clays. Can. Geotech. J. 26:199–209
734 34. Graham Y and (1993) Equivalent Times and One Dimensional Elastic Viscoplastic
735 Modelling of Time Dependent Stress Strain Behaviour of Clays
736 35. Yin JH, Graham J (1999) Elastic viscoplastic modelling of the time-dependent stress-
737 strain behaviour of soils. Can Geotech J 36(4):736–745. https://doi.org/10.1139/t99-
738 042
739 36. Yin JH, Zhu JG, Graham J (2002) A new elastic viscoplastic model for time-dependent
740 behaviour of normally and overconsolidated clays: Theory and verification. Can
741 Geotech J 39(1):157–173. https://doi.org/10.1139/t01-074
742 37. Chen ZJ, Feng W, Li A, et al (2023) Experimental and molecular dynamics studies on
743 the consolidation of Hong Kong marine deposits under heating and vacuum
744 preloading. Acta Geotech 182569–2583. https://doi.org/10.1007/s11440-022-01735-x
745 38. Chen ZJ, Feng WQ, Yin JH (2021) A new simplified method for calculating short-
746 term and long-term consolidation settlements of multi-layered soils considering creep
747 limit. Comput Geotech 138(May):104324.
748 https://doi.org/10.1016/j.compgeo.2021.104324
749 39. Chen ZJ, Feng WQ, Yin JH, Shi XS (2023) Finite element model and simple method
750 for predicting consolidation displacement of soft soils exhibiting creep underneath
751 embankments in 2-D condition. Acta Geotech 18(5):2513–2528.
752 https://doi.org/10.1007/s11440-022-01741-z
753 40. Asaoka (1978) Observational procedure of settlement prediction. Soils Found
754 18(4):87–101. https://doi.org/https://doi.org/10.3208/sandf1972.18.4_87
755 41. Tan TS, Inoue T, Lee SL (1991) Hyperbolic method for consolidation analysis. J
756 Geotech Eng 117(11):1723–1737. https://doi.org/10.1061/(ASCE)0733-

9410(1993)119:1(190)

42. Tan SA (1994) Hyperbolic method for settlements in clays with vertical drains. Can Geotech J 31(1):125–131. https://doi.org/10.1139/t94-014

43. Tan SA (1993) Ultimate settlement by hyperbolic plot for clays with vertical drains. J Geotech Eng 119(5):950–956. https://doi.org/https://doi.org/10.1061/(ASCE)0733-9410(1993)119:5(950)

44. Barron RA (1948) Consolidation of fine-grained soils by drain wells by drain wells. Trans Am Soc Civ Eng 113(1):718–742

45. Zhu W, Yan J, Yu G (2018) Vacuum preloading method for land reclamation using hydraulic filled slurry from the sea: A case study in coastal China. Ocean Eng 152(February):286–299. https://doi.org/10.1016/j.oceaneng.2018.01.063

46. Xu K (2011) On a slow moving slope in Hong Kong. PhD thesis, The University of Hong Kong

47. Chai J, Carter J, Liu M (2014) Methods of vacuum consolidation and their deformation analyses. Proc Inst Civ Eng Gr Improv 167(1):35–46. https://doi.org/10.1680/grim.13.00017

48. Cognon J, Juran I, Thevanayagam S (1994) Vacuum consolidation technology-principles and field experience. In: Proceedings of the Conference on Vertical and Horizontal Deformations of Foundations and Embankments In Part 2. pp 1237–1248

49. Mikasa M (1965) The consolidation of soft clay. In: Japan Society of Civil Engineering, Tokyo. pp 21–26

50. Walker R, Indraratna B (2009) Consolidation analysis of a stratified soil with vertical and horizontal drainage using the spectral method. Géotechnique 59(5):439–449. https://doi.org/10.1680/geot.2007.00019

51. Walker R, Indraratna B, Sivakugan N (2009) Vertical and radial consolidation analysis

of multilayered soil using the spectral method. J Geotech Geoenvironmental Eng 135(5):657–663. https://doi.org/10.1061/(asce)gt.1943-5606.0000075

52. Chung SG, Kweon HJ, Jang WY (2014) Observational method for field performance of prefabricated vertical drains. Geotext Geomembranes 42(4):405–416. https://doi.org/10.1016/j.geotexmem.2014.06.005

53. He GF, Zhang P, Yin ZY, et al (2023) Multi-fidelity data-driven modelling of rate-dependent behaviour of soft clays. Georisk 17(1):64–76. https://doi.org/10.1080/17499518.2022.2149815

54. Zhao S, Tan D, Lin S, et al (2023) A deep learning-based approach with anti-noise ability for identification of rock microcracks using distributed fibre optic sensing data. Int J Rock Mech Min Sci 170(March):105525. https://doi.org/10.1016/j.ijrmms.2023.105525

55. Chu J, Raju V (2012) Prefabricated vertical drains. Ground Improvement (Kirsch K and Bell A (eds)), 3rd edn. CRC Press, Florida, USA. 87–167

56. Feng WQ, Li C, Yin JH, et al (2019) Physical model study on the clay–sand interface without and with geotextile separator. Acta Geotech 14(6):2065–2081. https://doi.org/10.1007/s11440-019-00763-4

57. Feng WQ, Tan DY, Yin JH, et al (2020) Experimental and numerical studies on the performances of stone column and sand compaction pile–reinforced Hong Kong marine clay. Int J Geomech 20(8):1–6. https://doi.org/10.1061/(asce)gm.1943-5622.0001739

58. Shi XS, Liu K, Yin JH (2021) Effect of initial density, particle shape, and confining stress on the critical state behavior of weathered gap-graded granular soils. J Geotech Geoenvironmental Eng 147(2):04020160. https://doi.org/10.1061/(asce)gt.1943-5606.0002449

59. Slocombe BC, Bell AL, Baez JI (2000) The densification of granular soils using vibro methods. Géotechnique 50(6):715–725. https://doi.org/10.1680/geot.2000.50.6.715

60. Wang HL, Yin ZY (2021) Unconfined compressive strength of bio-cemented sand: state-of-the-art review and MEP-MC-based model development. J Clean Prod 315(June):128205. https://doi.org/10.1016/j.jclepro.2021.128205

61. Xu DS, Yan JM, Liu Q (2021) Behavior of discrete fiber-reinforced sandy soil in large-scale simple shear tests. Geosynth Int 28(6):598–608. https://doi.org/10.1680/jgein.21.00007

62. Bergado D, Shin E, Park J (2007) Improvement of consolidation characteristics around PVD using the thermal method. J Korean Geotech Soc 23(10):5–11

63. Wang H, Chen R (2019) Estimating static and dynamic stresses in geosynthetic-reinforced pile-supported track-bed under train moving loads. J Geotech Geoenvironmental Eng 145(7):1–14. https://doi.org/10.1061/(asce)gt.1943-5606.0002056

64. Zhu HH, Yin JH, Yeung AT, Jin W (2011) Field pullout testing and performance evaluation of GFRP soil nails. J Geotech Geoenvironmental Eng 137(7):633–642. https://doi.org/10.1061/(asce)gt.1943-5606.0000457

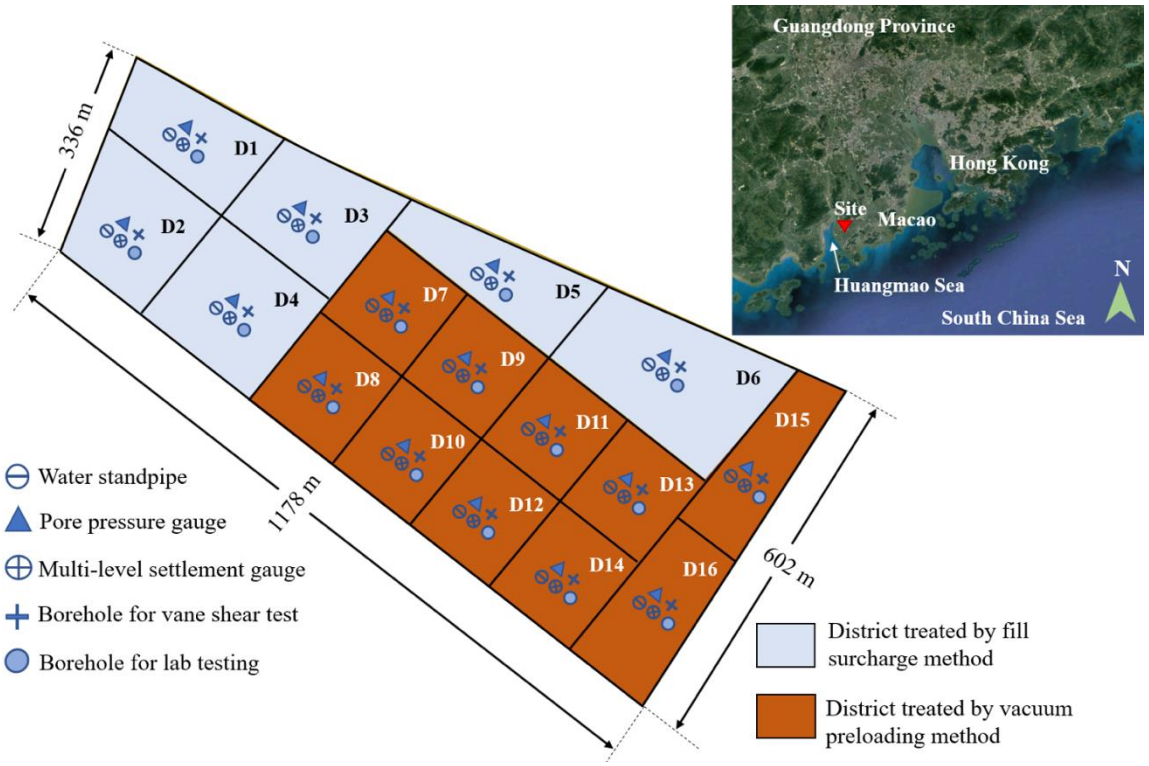

(a)

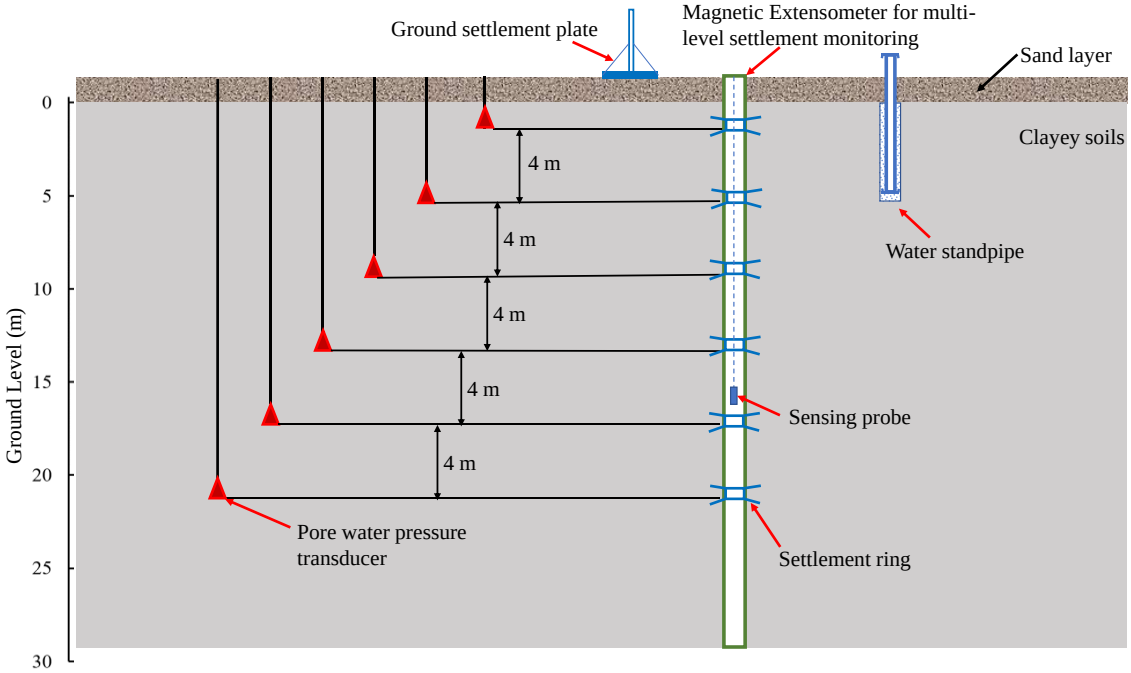

(b)

Fig. 1 (a) Layout and instrumentation of studied area for ground improvement; and (b) cross-sectional view of typical instruments

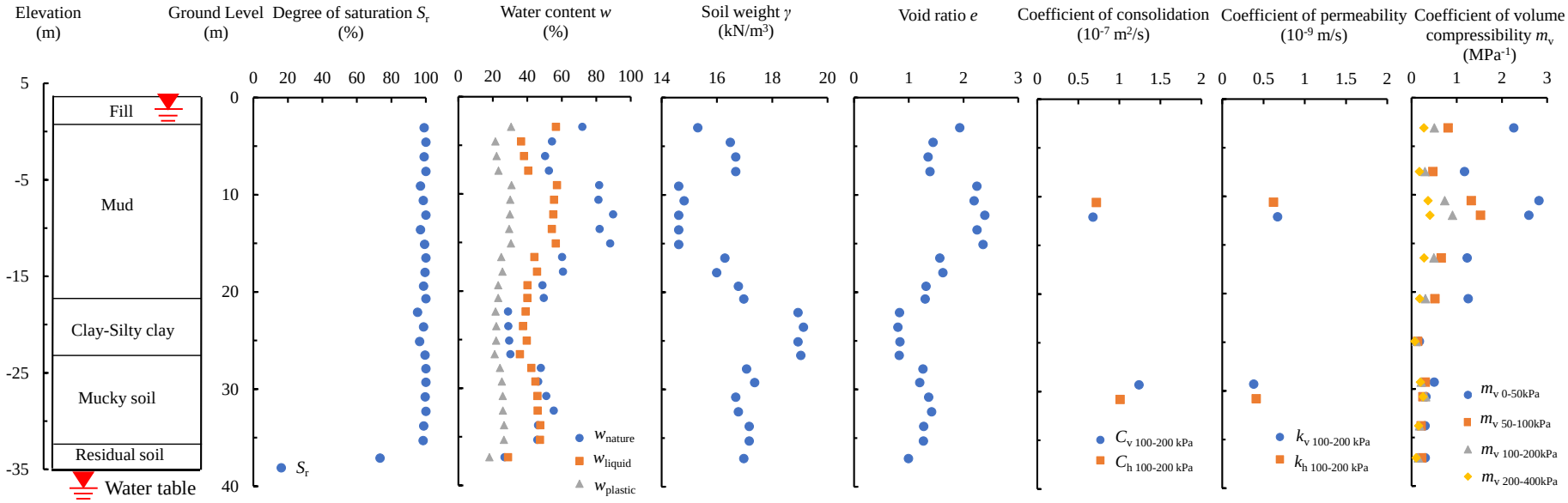

Fig. 2 Illustration of soil profile and basic properties of soils

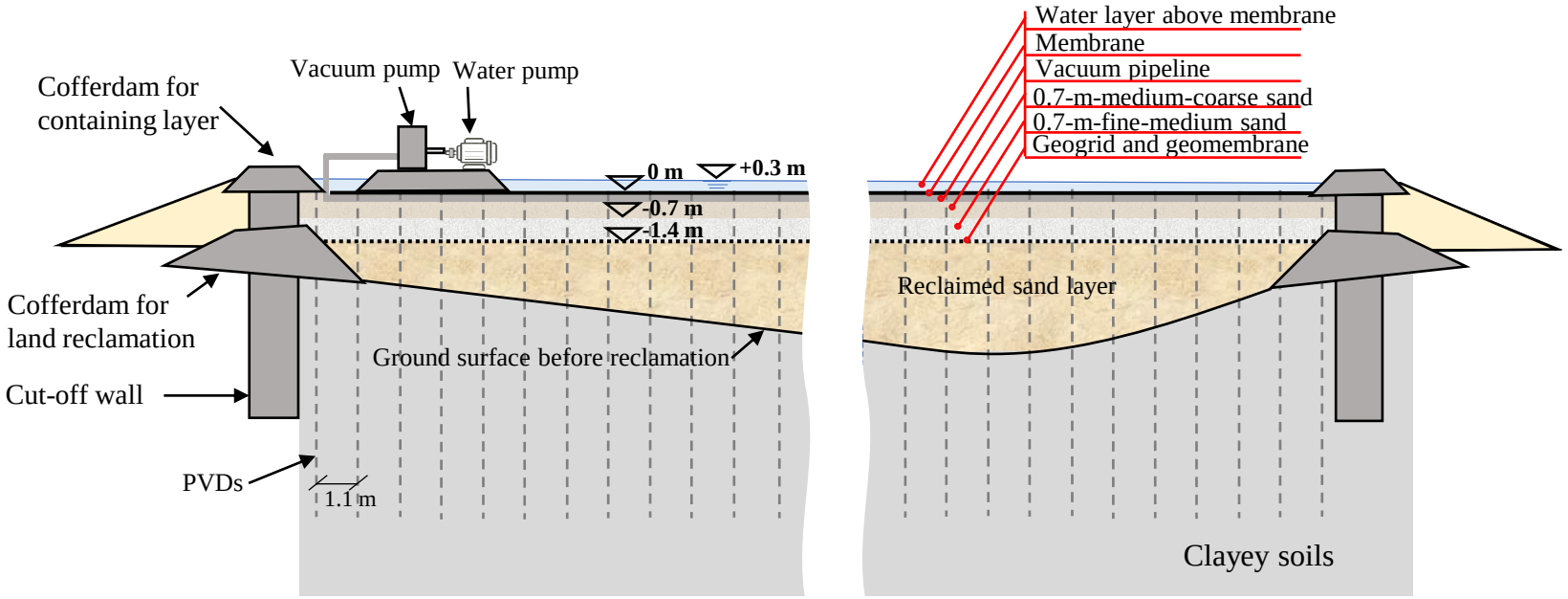

835

836 **Fig. 3** Schematic layout of the vacuum preloading method

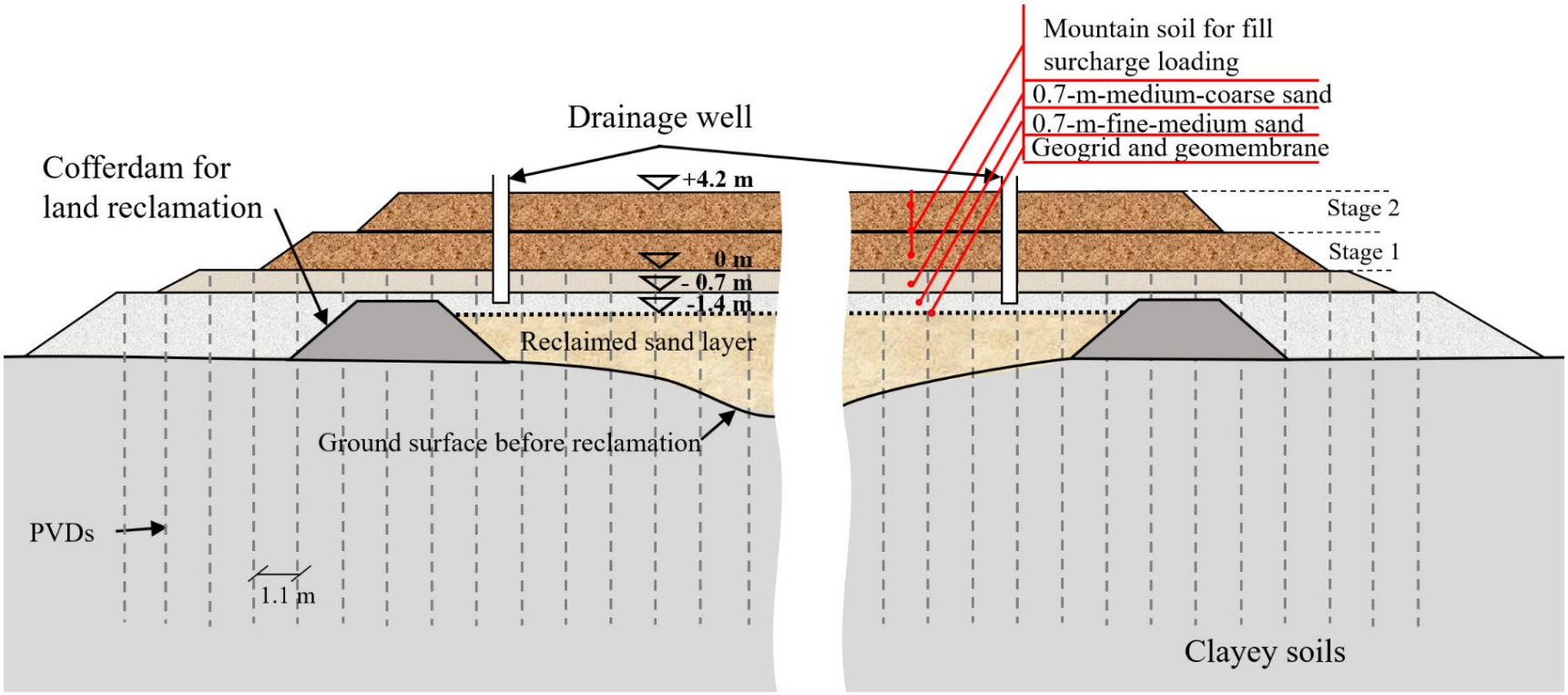

Fig. 4 Schematic layout of the fill surcharge method

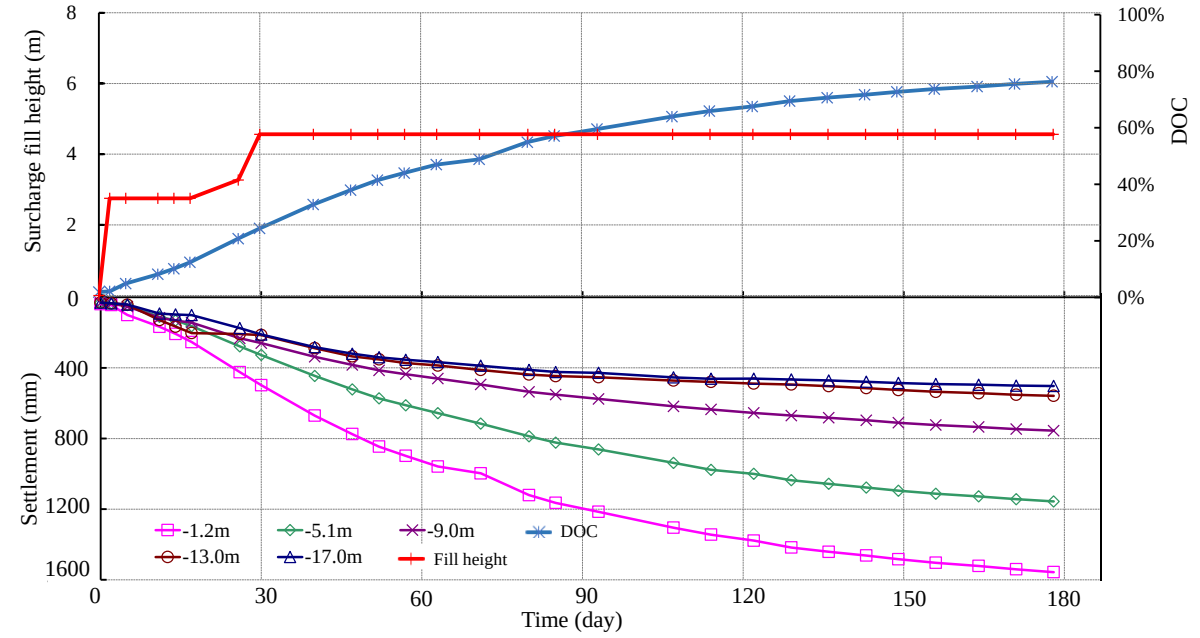

(a)

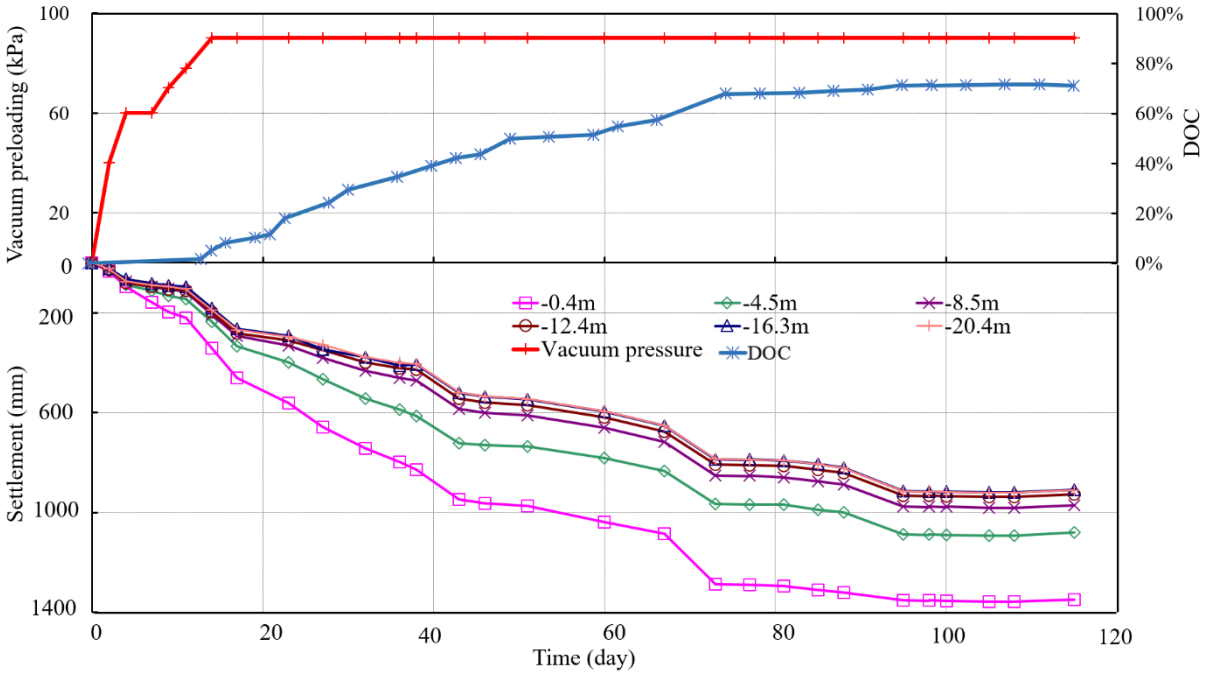

(b)

Fig. 5 Settlements measured at different depths plotted against time duration of (a) Zone D1 improved by fill surcharge method; and (b) Zone D8 improved by vacuum preloading method

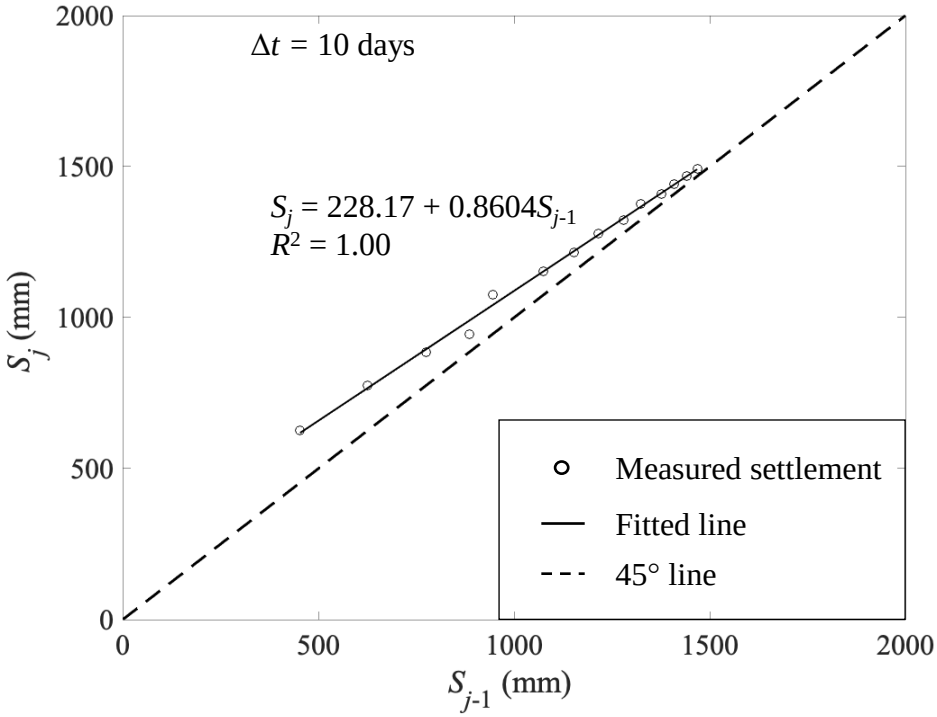
Δt = 10 days
S_j = 228.17 + 0.8604S_{j-1}
R^2 = 1.00
Measured settlement
Fitted line
45° line
S_j (mm)
S_{j-1} (mm)
0
500
1000
1500
2000

(a)

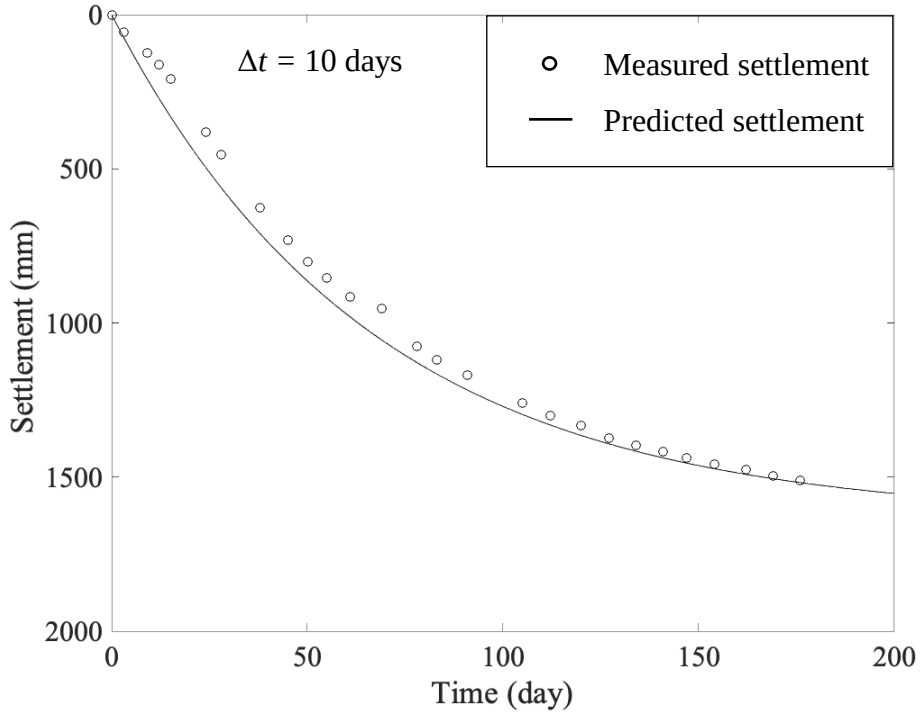
Δt = 10 days
Measured settlement
Predicted settlement
Settlement (mm)
Time (day)
0
50
100
150
200
500
1000
1500
2000

(b)

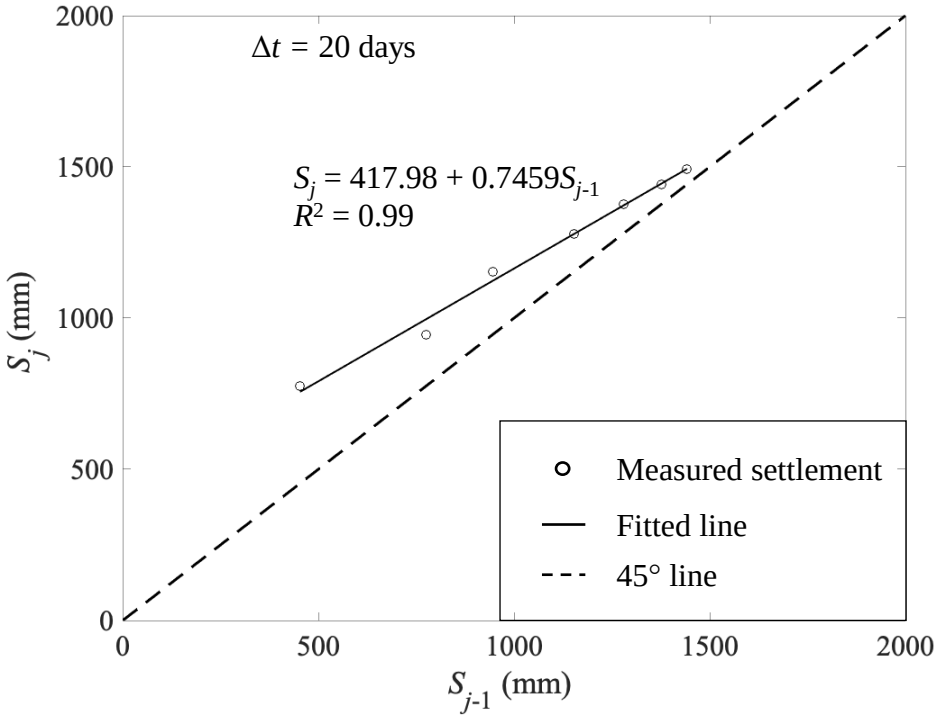

854

855 (c)

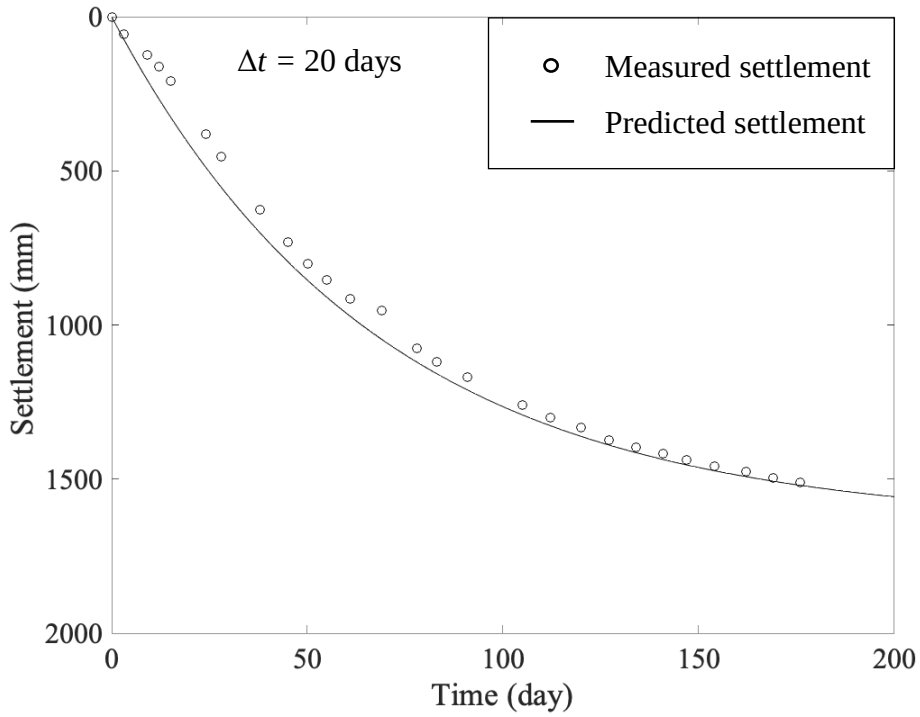

856

857 (d)

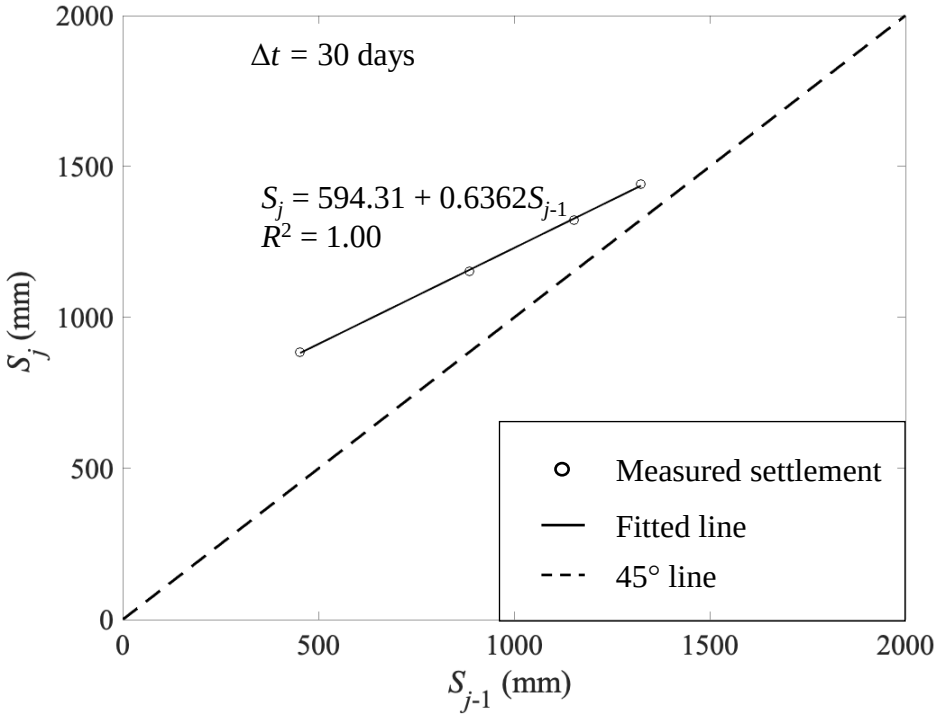

(e)

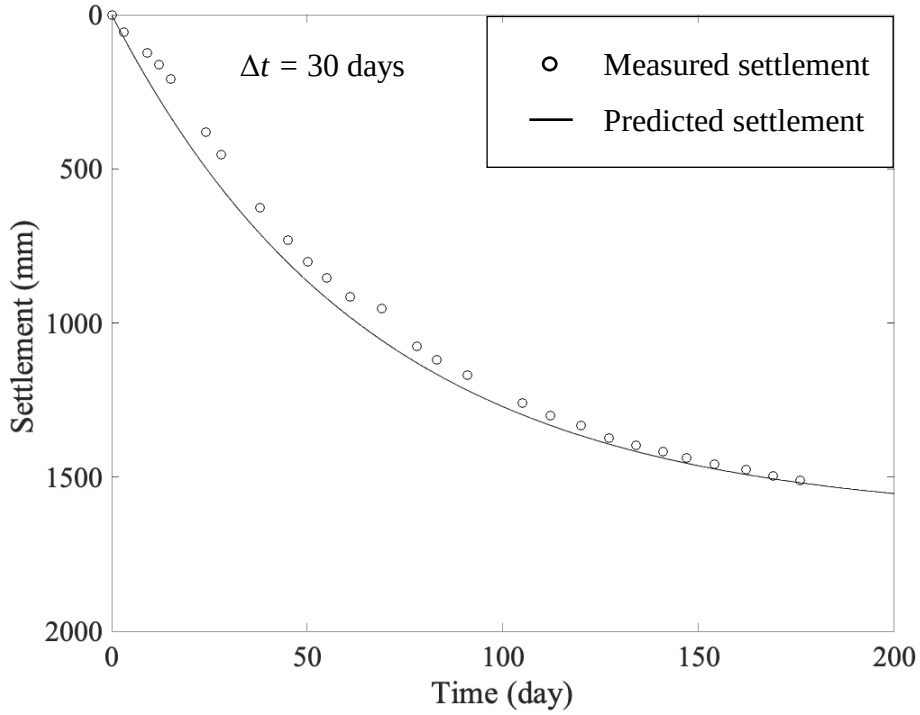

(f)

Fig. 6 Plots for Zone D1 based on the Asaoka method: (a) $S_j - S_{j-1}$ for Δt = 10 days; (b) settlement curve for Δt = 10 days; (c) $S_j - S_{j-1}$ for Δt = 20 days; (d) settlement curve for Δt = 20 days; (e) $S_j - S_{j-1}$ for Δt = 30 days; and (f) settlement curve for Δt = 30 days

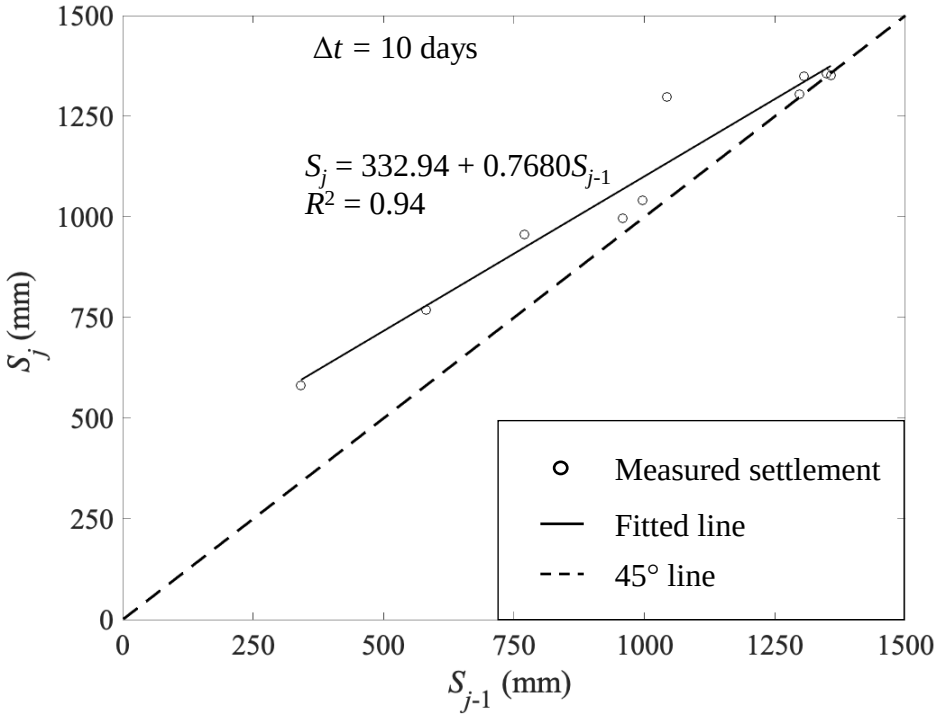
Δt = 10 days
S_j = 332.94 + 0.7680S_{j-1}
R^2 = 0.94
Measured settlement
Fitted line
45° line
S_j (mm)
S_{j-1} (mm)
0
250
500
750
1000
1250
1500

(a)

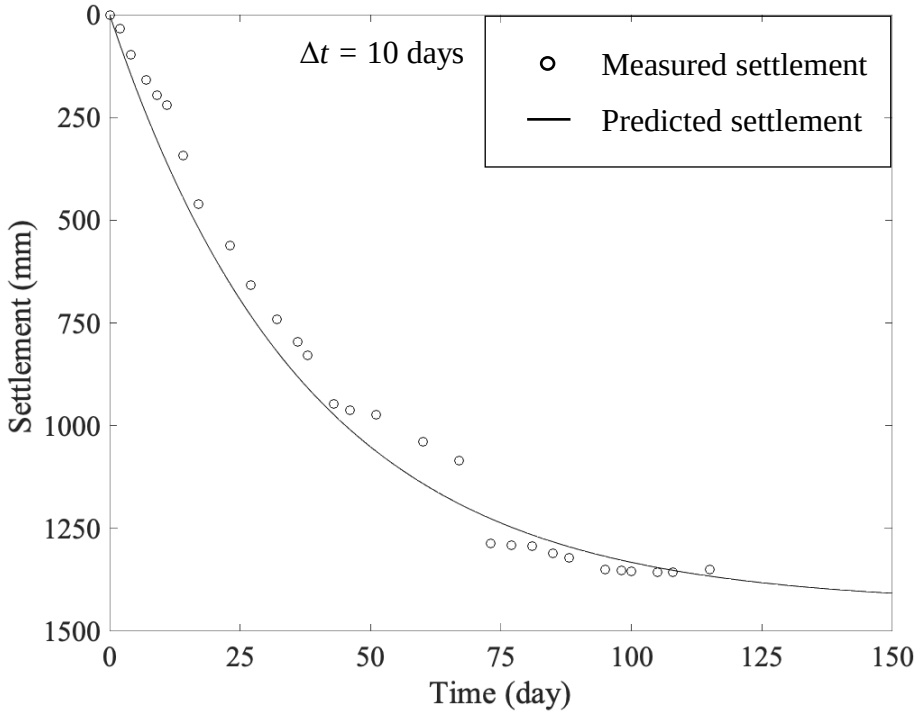
Δt = 10 days
Measured settlement
Predicted settlement
Settlement (mm)
Time (day)
0
25
50
75
100
125
150
250
500
750
1000
1250
1500

(b)

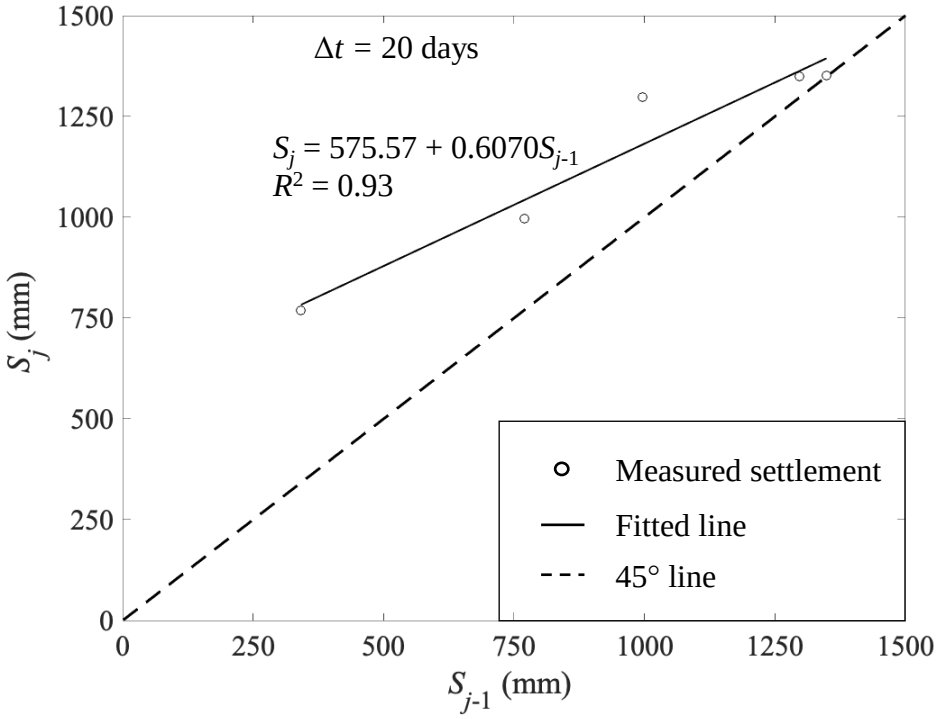

870

871 (c)

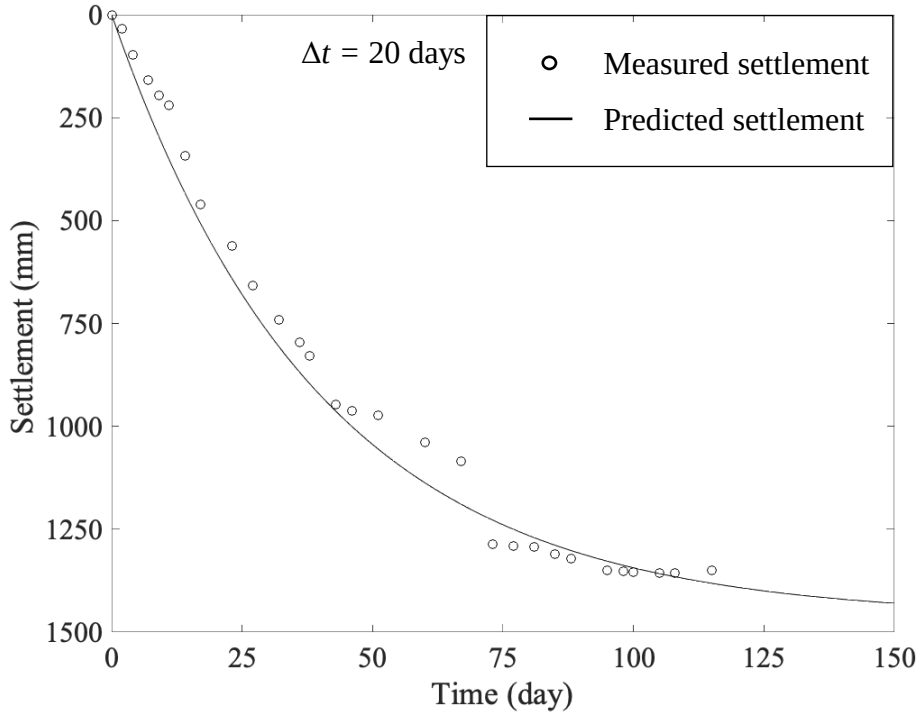

872

873 (d)

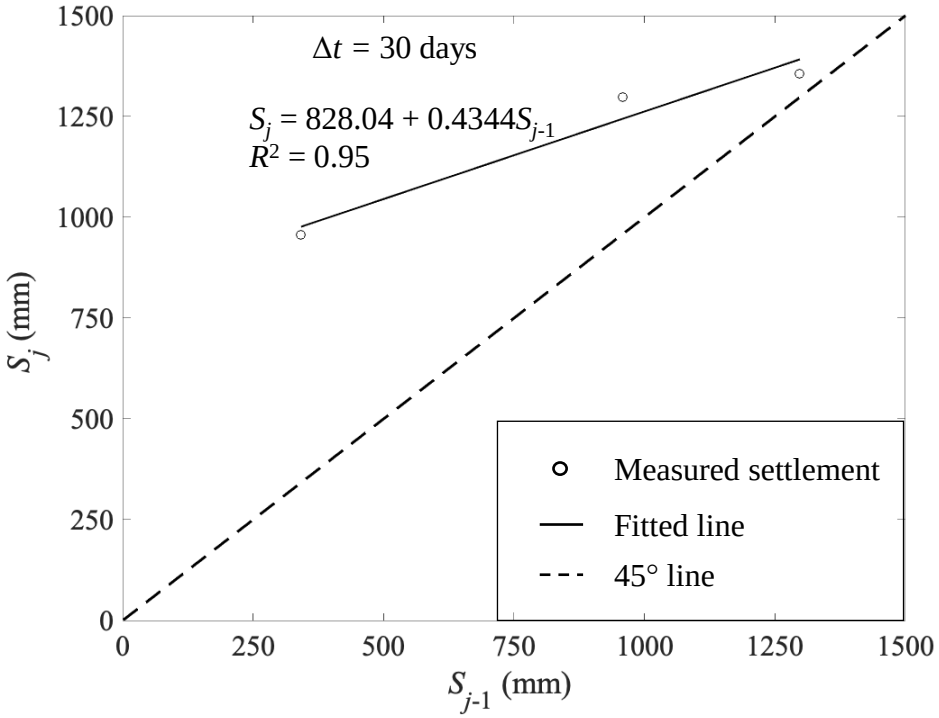

(e)

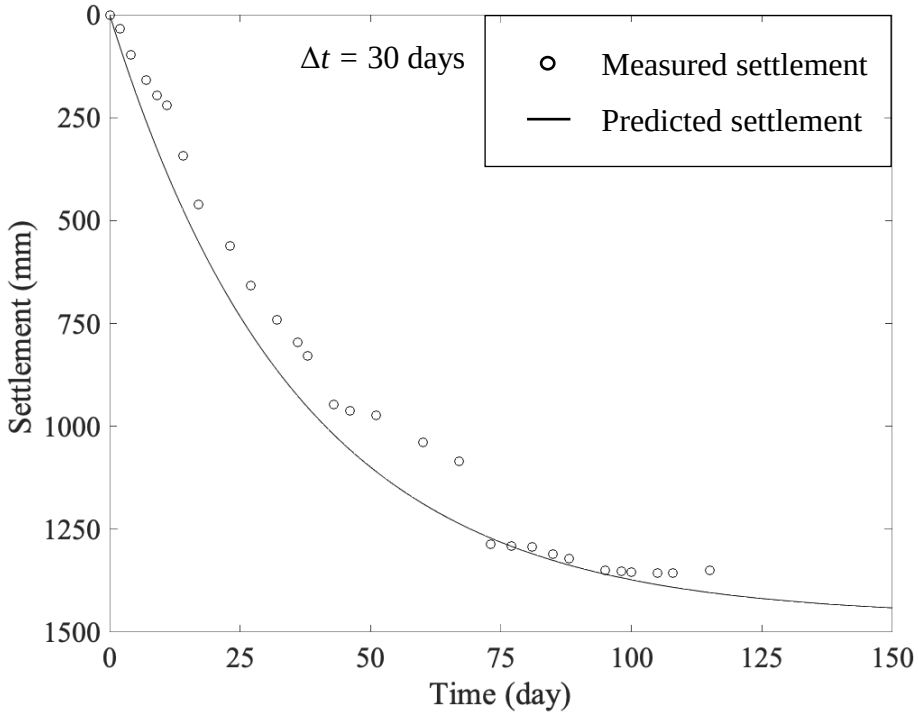

(f)

Fig. 7 Plots for Zone D8 based on the Asaoka's method: (a) $S_j - S_{j-1}$ for Δt = 10 days; (b) settlement curve for Δt = 10 days; (c) $S_j - S_{j-1}$ for Δt = 20 days; (d) settlement curve for Δt = 20 days; (e) $S_j - S_{j-1}$ for Δt = 30 days; and (f) settlement curve for Δt = 30 days

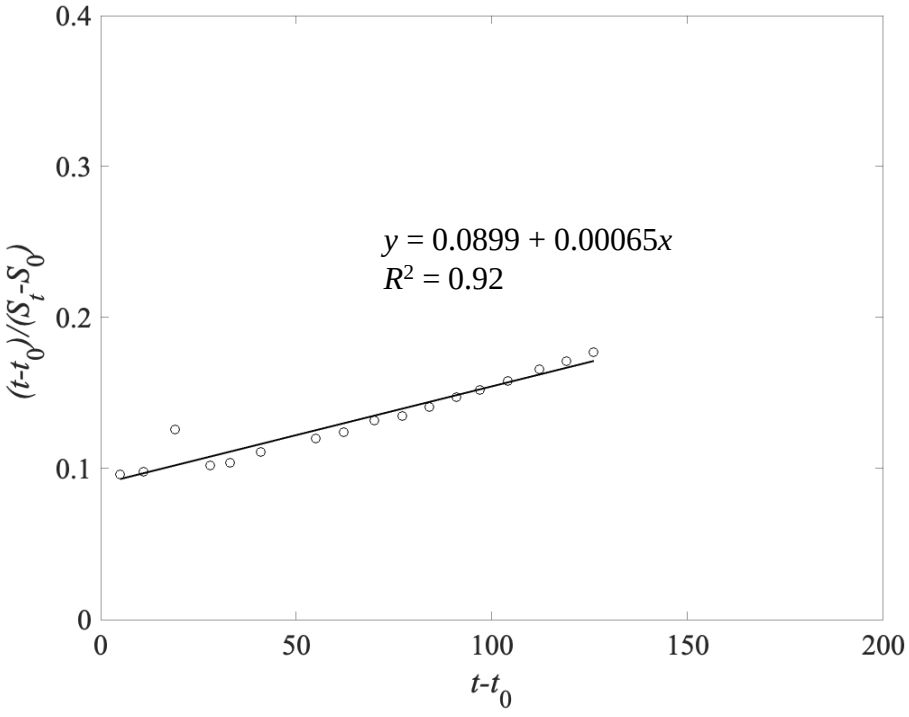

882

883 (a)

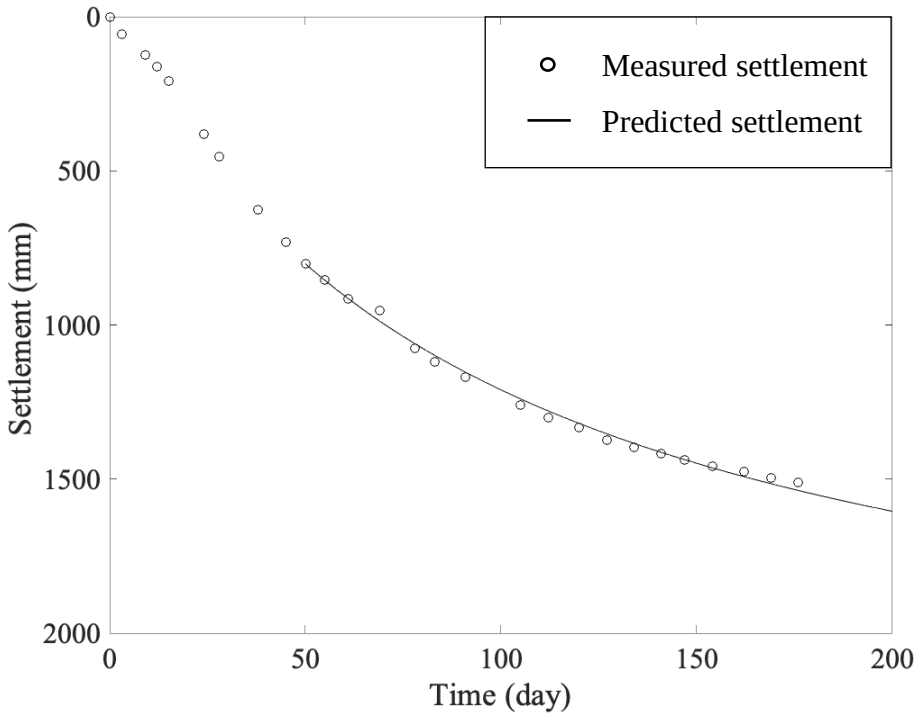

884

885 (b)

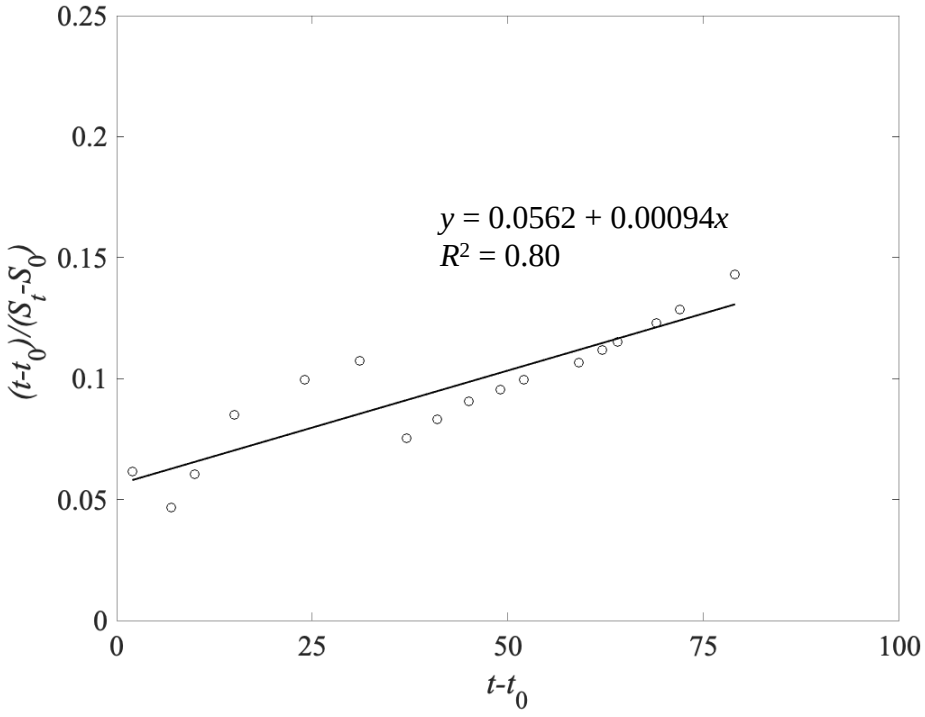

(c)

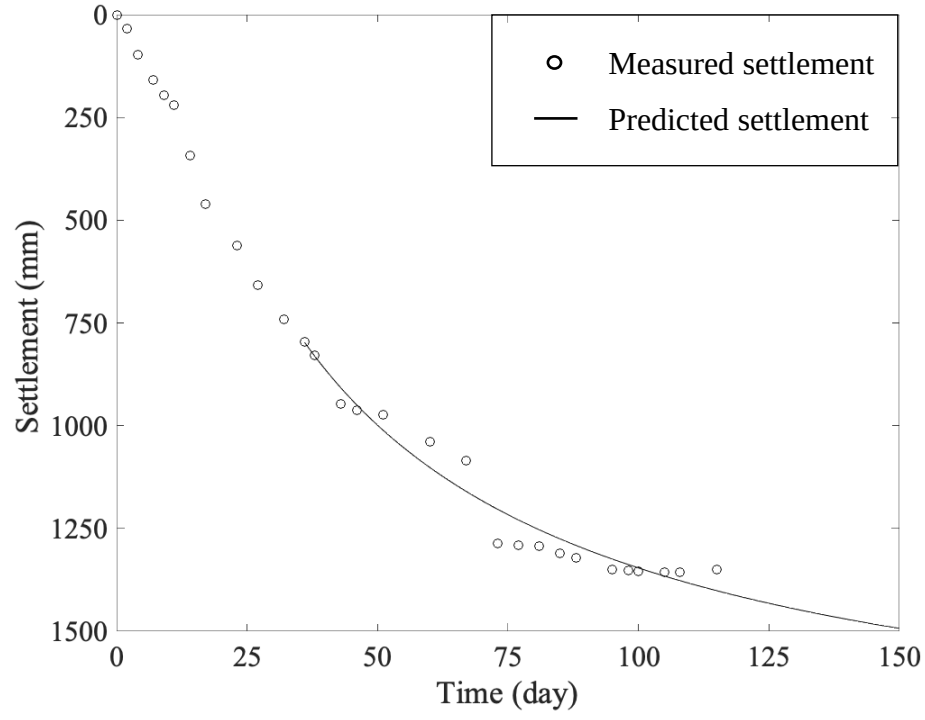

(d)

Fig. 8 Plots for Zones D1 and D8 based on the hyperbolic curve method: (a) $(t - t_0) / (S_t - S_0)$ for Zone D1; (b) settlement curve for Zone D1; (c) $(t - t_0) / (S_t - S_0)$ for Zone D8; and (d)

settlement curve for Zone D8

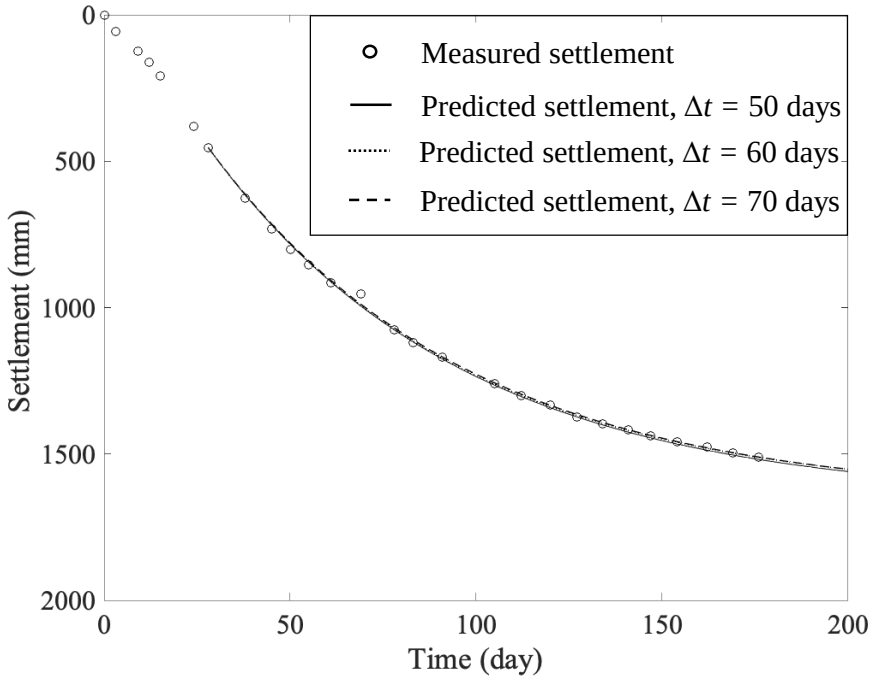

(a)

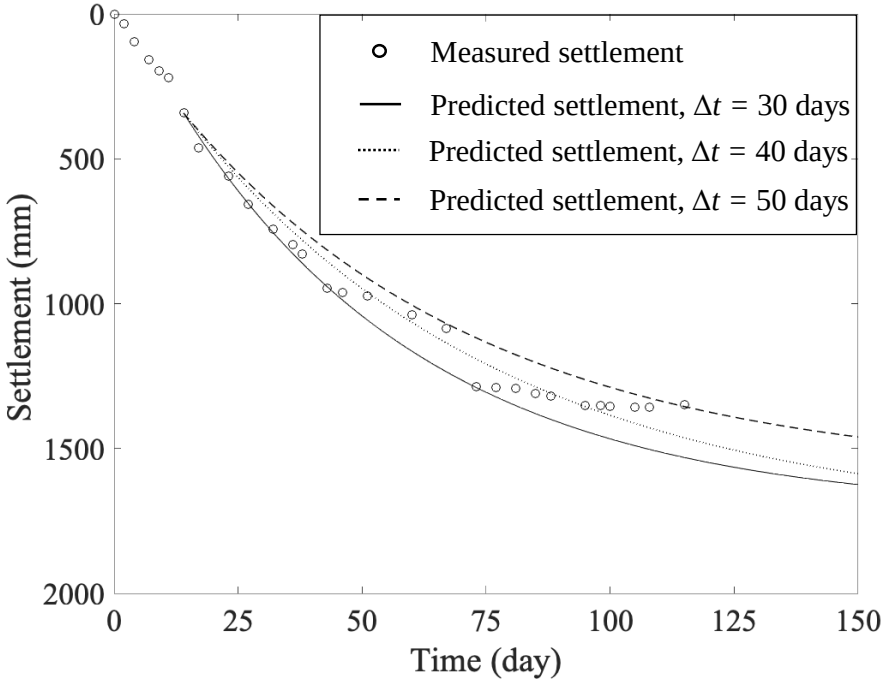

(b)

Fig. 9 Plots for Zones D1 and D8 based on the exponential curve method: (a) settlement curves for Zone D1 for time intervals of 50, 60, and 70 days; and (b) settlement curves for Zone D8 for time intervals of 30, 40, and 50 days

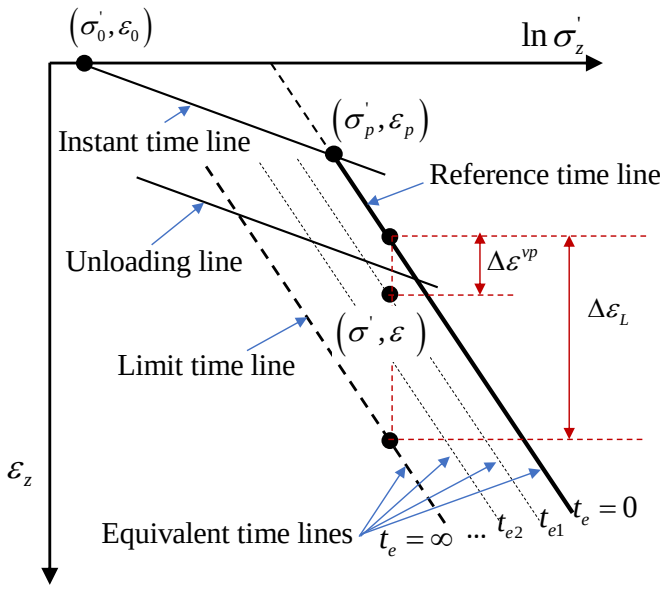

901

902 **Fig. 10** The schematic diagram of the 1-D nonlinear EVP model

903

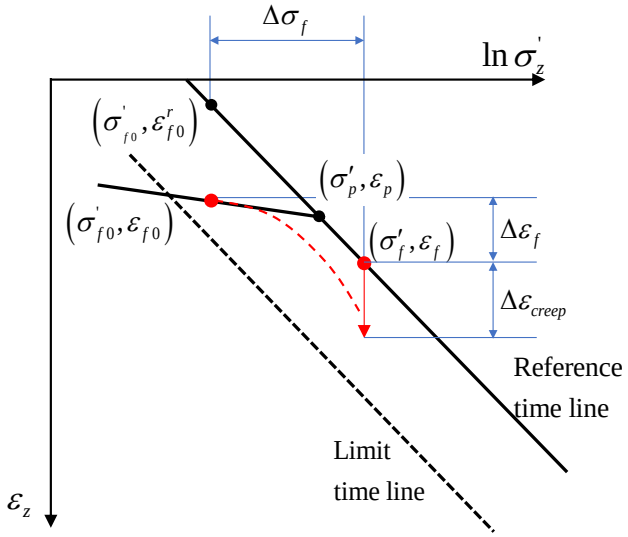

(a)

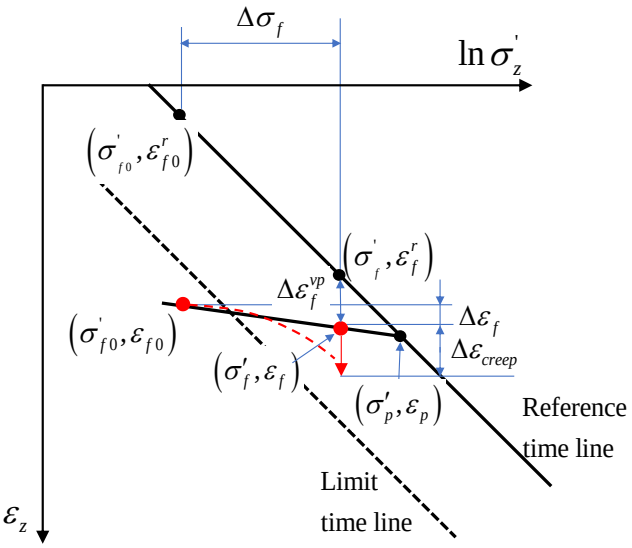

(b)

Fig. 11 The schematic diagram of creep calculation when the final stress-strain of soil $\left(\sigma_f', \varepsilon_f\right)$ is at: (a) normally consolidation state; and (b) over-consolidation state

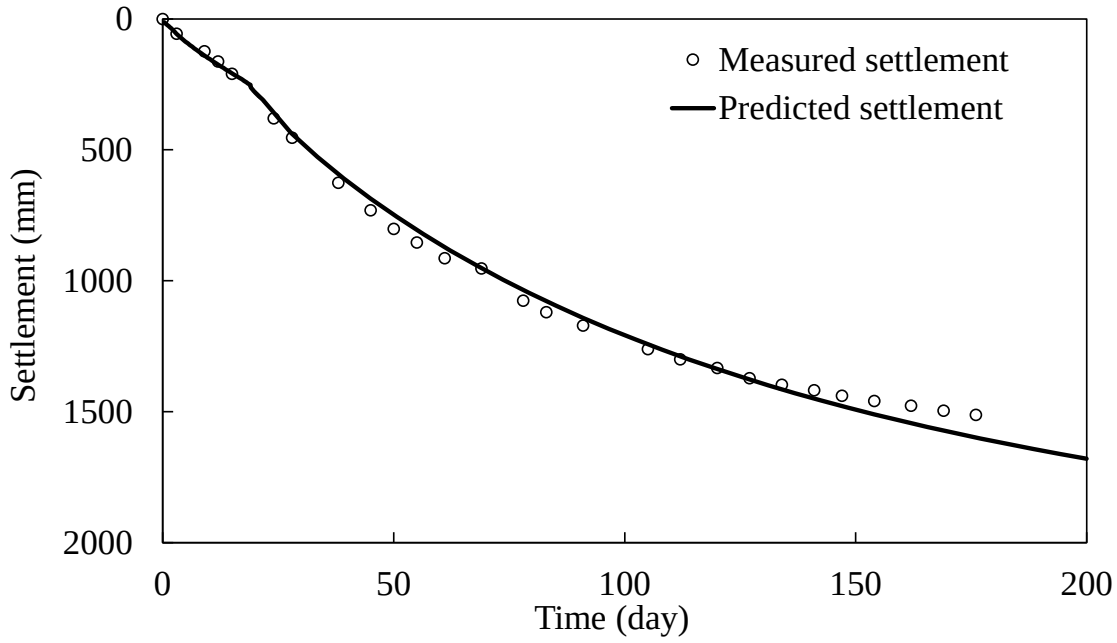

912

913 (a)

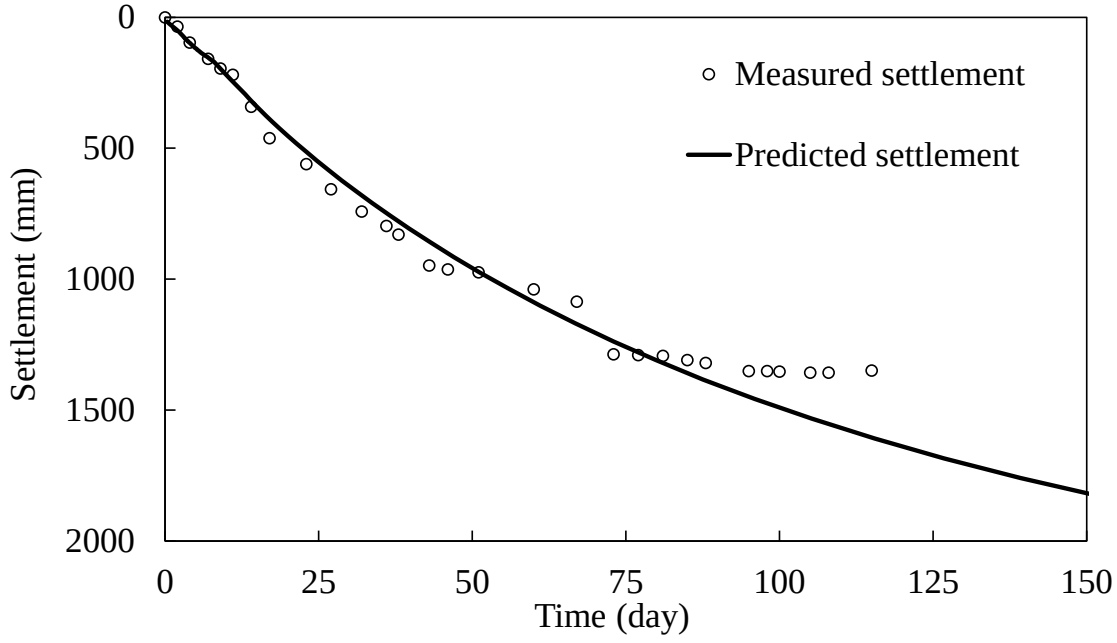

914

915 (b)

916 **Fig. 12** Settlement curves for Zones D1 and D8 based on the new simplified B method: (a)
917 Zone D1; and (b) Zone D8

918

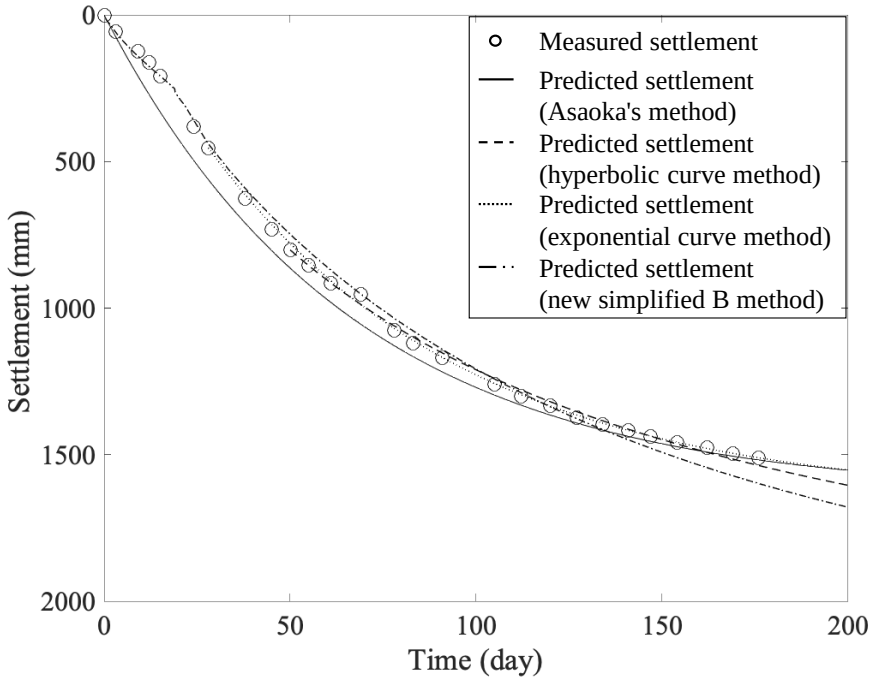

(a)

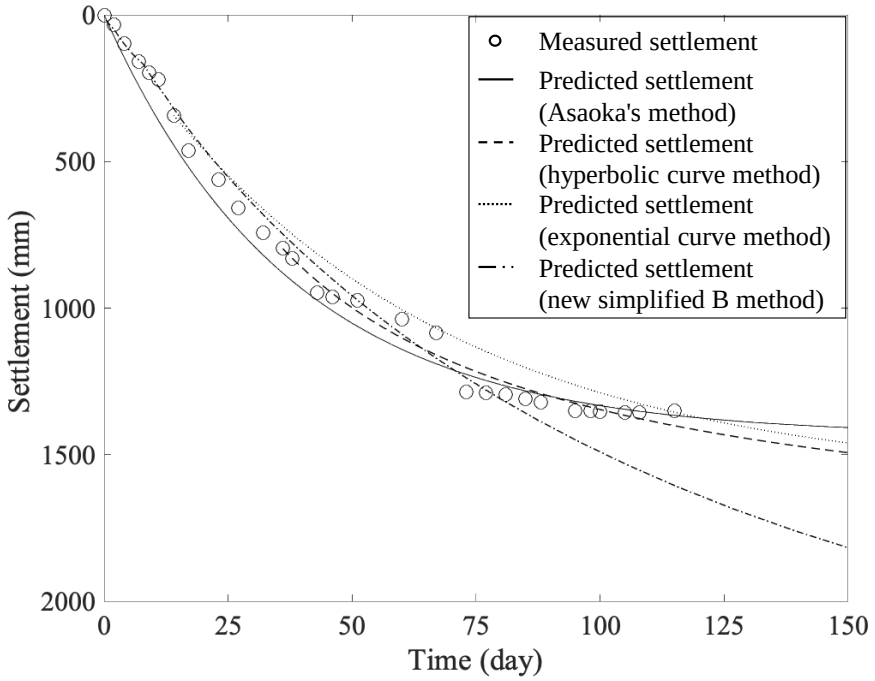

(b)

Fig. 13 Comparison of measured and predicted settlement results based on different methods in different zones: (a) Zone D1; and (b) Zone D8

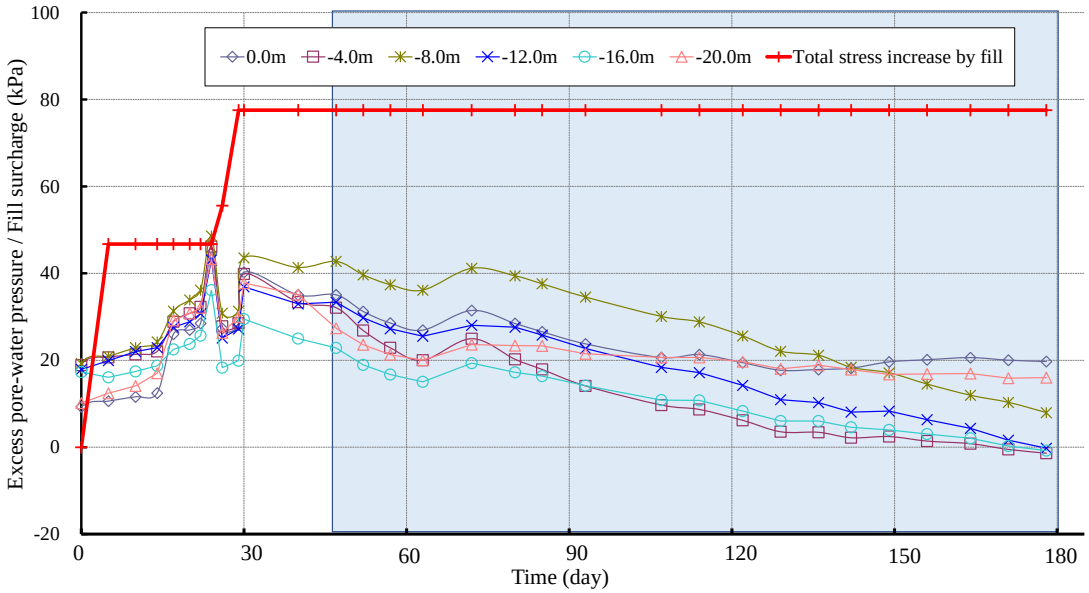

926

927 (a)

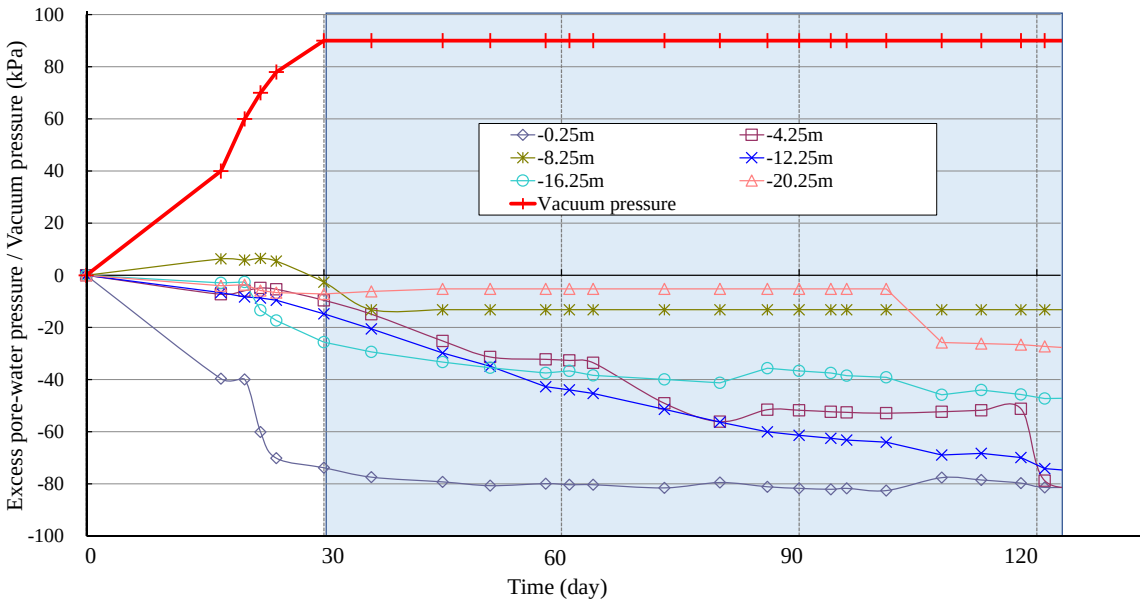

928

929 (b)

930 **Fig. 14** Excess pore-water pressures measured at different depths plotted against time duration
931 of (a) (a) Zone D1 improved by fill surcharge method; and (b) Zone D8 improved by vacuum
932 preloading method

933

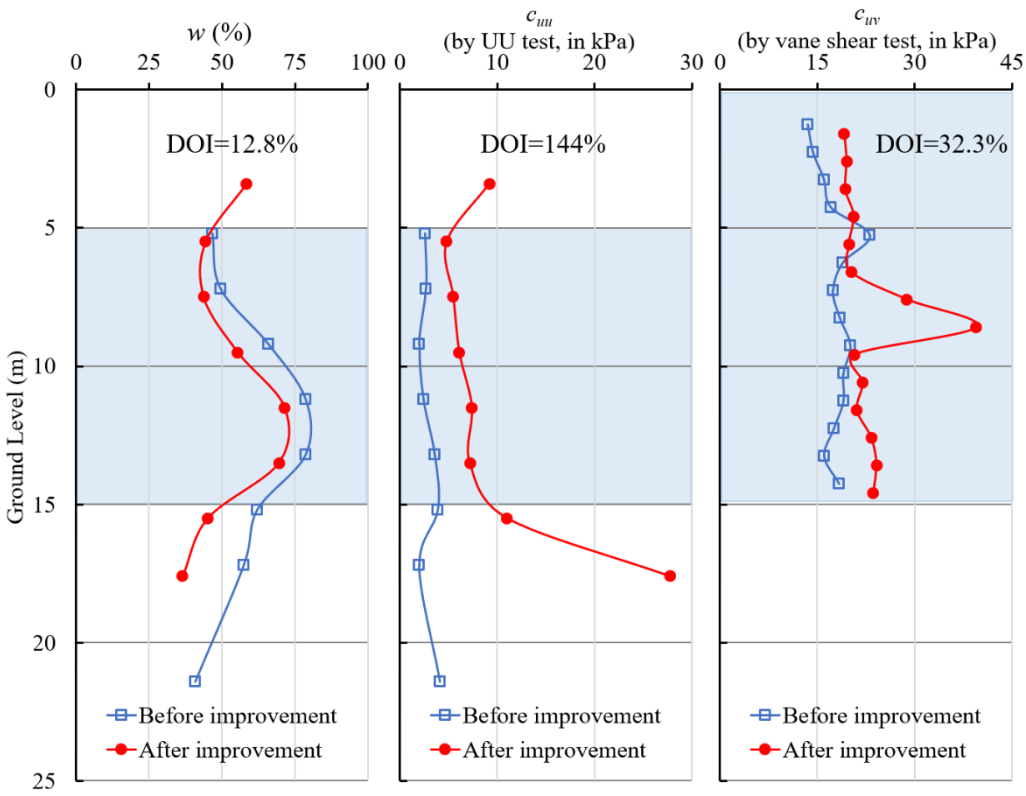

(a)

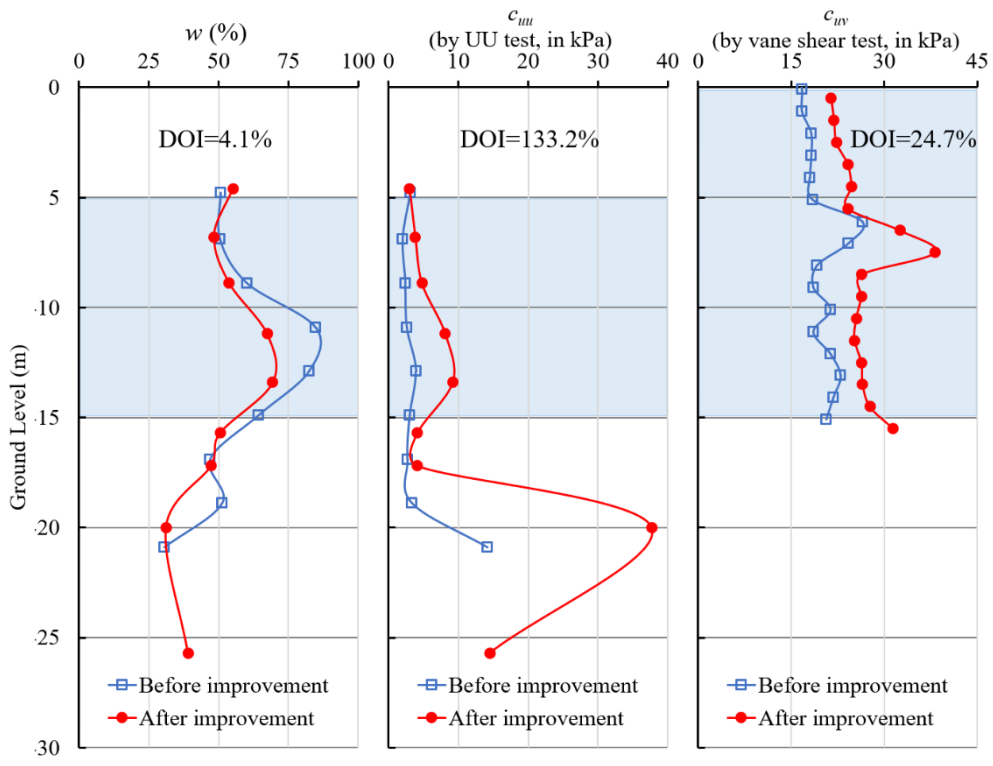

(b)

Fig. 15 Water content (w), cohesion (c_{uu}), and shear strength (c_{uv}) before and after the improvement of (a) vacuum preloading method and (b) fill surcharge method

940 **Table 1** Review of the state-of-the-art soil improvement techniques

Type of method	Representative specific techniques	Relevant studies or cases
Consolidation acceleration	Fill-surcharge (with or without vertical drain), vacuum preloading with vertical drain or/and horizontal drain, electro-osmosis	Bo et al. [24]; Chai et al. [47]; Chu and Raju [55]; Feng et al. [56]
Particle densification	Stone columns, sand compaction piles, dynamic compaction, vibro-compaction	Feng et al. [57]; Shi et al. [58]; Slocombe et al. [59]
Admixtures	Mix-in-place piles, bio-cementation, fibers	Wang and Yin [60]; Xu et al. [61]
Thermal	Heating, freezing	Bergado et al. [62]
Reinforcement	Soil nailing, geotextile and geomembrane	Wang and Chen [63]; Zhu et al. [64]

941

942 **Table 2** Predicted ultimate settlements and settlements at a measured period by the Asaoka's
943 method

Zone	Δt (days)	β_0 (mm)	β_1	S_∞ (mm)	S_t (mm)	S_m (mm)	Measured period (days)	Error (%)
D1	10	228.17	0.8604	1633.9	1518.1	1512.0	176	0.40
	20	417.98	0.7459	1645.1	1520.4			0.56
	30	594.31	0.6362	1633.6	1518.5			0.43
D8	10	332.94	0.7680	1435.0	1366.0	1349.5	115	1.22
	20	575.57	0.6070	1464.6.	1381.6			2.38
	30	828.04	0.4344	1463.9	1404.0			4.04

944

945 **Table 3** Predicted ultimate settlements and settlements at a measured period by the hyperbolic
946 curve method

Zone	t_0 (days)	S_0 (mm)	α	β	S_∞ (mm)	S_t (mm)	S_m (mm)	Measured period (days)	Error (%)
D1	50	801.5	0.0899	0.00065	2349.2	1537.1	1512.0	176	1.66
D8	36	797.0	0.0562	0.00094	1856.8	1401.4	1349.5	115	3.85

947

948 **Table 4** Predicted ultimate settlements and settlements at a measured period by the exponential
949 curve method

Zone	t_i (days)	Δt (days)	β'	S_∞ (mm)	S_t (mm)	S_m (mm)	Measured period (days)	Error (%)
D1	28	50	0.0145	1659.1	1518.7	1512.0	176	0.44
		60	0.0146	1648.5	1511.6			0.03
		70	0.0144	1652.8	1510.6			0.09
D8	14	30	0.0198	1718.0	1531.1	1349.5	115	13.46
		40	0.0155	1759.3	1462.8			8.40
		50	0.0164	1595.7	1355.3			0.43

Table 5 Soil parameters adopted in the new simplified B method for predicting settlements in different zones

Zone	Soil type	Layer No.	H (m)	OCR	γ (kN/m^3)	κ	λ	ψ_0	$\Delta\varepsilon_L$	t_0 (h)	$1+e_0$	k_v (m/y)
D1	Mud	1	5.0	1.00	15.9	0.0343	0.257	0.008	0.027	24	2.785	0.02334
		2	5.0	1.00	15.9	0.0343	0.257	0.008	0.027	24	2.785	0.02334
		3	4.9	1.00	15.9	0.0343	0.257	0.008	0.027	24	2.785	0.02334
	Clay-Silty clay	4	2.7	1.00	19.0	0.0116	0.257	0.001	0.005	24	1.849	0.01703
	Mucky soil	5	2.2	1.11	17.9	0.0230	0.257	0.001	0.003	24	2.157	0.0164
	Clay-Silty clay	6	2.2	1.00	19.2	0.0106	0.257	0.001	0.004	24	1.799	0.01367
	Mucky soil	7	1.8	1.00	18.6	0.0165	0.257	0.003	0.007	24	2.116	0.01072
D8	Mud	1	4.0	1.00	15.9	0.0343	0.257	0.008	0.027	24	2.785	0.02334
		2	4.0	1.00	15.9	0.0343	0.257	0.008	0.027	24	2.785	0.02334
		3	5.0	1.00	15.9	0.0343	0.257	0.008	0.027	24	2.785	0.02334
		4	5.1	1.00	15.9	0.0343	0.257	0.008	0.027	24	2.785	0.02334
	Clay-Silty clay	5	3.0	1.00	19.2	0.0106	0.079	0.001	0.004	24	1.799	0.01367
		6	3.2	1.00	19.2	0.0106	0.079	0.001	0.004	24	1.799	0.01367
	Mucky soil	7	4.0	1.00	18.6	0.0165	0.108	0.003	0.007	24	2.116	0.01072
		8	4.9	1.00	18.6	0.0165	0.108	0.003	0.007	24	2.116	0.01072

Table 6 Results of predicted ultimate settlements by different methods

Zone	Asaoka's method	Hyperbolic curve method	Exponential curve method	New simplified B method
D1	1633.9 mm	2349.2 mm	1652.8 mm	2346.3
D8	1435.0 mm	1856.8 mm	1595.7 mm	2755.0